NASA Technical Paper 3029

July 1990

# Low Velocity Instrumented Impact Testing of Four New Damage Tolerant Carbon/Epoxy Composite Systems



D. G. Lance
and A. T. Nettles



NASA

# DISCLAIMER NOTICE

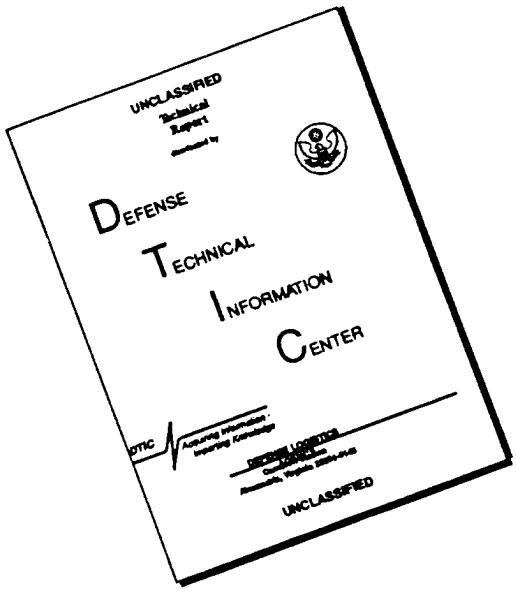


THIS DOCUMENT IS BEST QUALITY AVAILABLE. THE COPY FURNISHED TO DTIC CONTAINED A SIGNIFICANT NUMBER OF PAGES WHICH DO NOT REPRODUCE LEGIBLY.

**NASA Technical Paper 3029**

1990

# Low Velocity Instrumented Impact Testing of Four New Damage Tolerant Carbon/Epoxy Composite Systems

D. G. Lance
and A. T. Nettles
*George C. Marshall Space Flight Center*
*Marshall Space Flight Center, Alabama*



National Aeronautics and Space Administration
Office of Management
Scientific and Technical Information Division

## TABLE OF CONTENTS

## LIST OF ILLUSTRATIONS

TECHNICAL PAPER

# LOW VELOCITY INSTRUMENTED IMPACT TESTING OF FOUR NEW DAMAGE TOLERANT CARBON/EPOXY COMPOSITE SYSTEMS

## I. INTRODUCTION

Since foreign object impact is a serious concern with carbon fiber reinforced polymeric materials, an effort has been made by some manufacturers to produce more damage tolerant resins. Furthermore, the newer generation of intermediate modulus carbon fibers have a much higher strain to failure, as well as a higher strength, than the earlier types of carbon fibers. Impregnating the improved fibers with the new damage resistant resins produces materials that can withstand a larger impact energy before material damage occurs.

Low-velocity instrumented impact methods have proven to be very useful in the study of damage tolerance of composite materials (Refs. 1–4). Such data as maximum force of impact, force-time graphs, and absorbed energy of impact can help the researcher characterize different composite materials for damage tolerance. Cross-sectioning of the specimen through the damage zone has also proven to yield practical information (Refs. 3,5–9). By utilizing this destructive analysis technique, the impact energies that cause matrix cracking, delaminations, and fiber breakage can all be identified. Furthermore, a comparison of the damage tolerance capabilities of various materials can be accomplished by observing which materials have the most amount of matrix cracking or larger extent of delaminations for a given impact energy. Comparisons can also be made between the visible surface damage and the internal damage identified by the cross-sectional examination.

Although a large amount of literature exists on impact damage testing and characterization of composite materials, data is lacking on the recently developed carbon fiber/epoxy resin systems. In order for the newer generation composites to be incorporated into high performance applications, much research needs to be accomplished to better understand the response of these composite materials to impacts. It is the purpose of this paper to present some preliminary experimental results on four new composite prepreg systems and compare these to an earlier generation fiber/resin system to see if there are indeed any improvements in impact resistance, and to characterize those improvements.

## II. MATERIALS AND EXPERIMENTAL METHODS

### 1. Material

Five different prepreg systems were used to construct the panels tested for this study. The T650/1939 and T650/1962 prepregs were manufactured by Amoco Performance Products. The IM7 carbon fibers were produced by Hercules Incorporated and impregnated by Amoco with the 1939 and 1962 resin systems. The T300 fibers were produced by Amoco and impregnated by Fiberite with the 934 resin.

The T300/394 was employed as a baseline material for this study because of the large data base already in existence on this material. The other materials were chosen because of their recent introduction into the market and promise of damage resistance. The T300 is an intermediate modulus fiber, and the 934 is a standard epoxy resin. The T650 and IM7 are intermediate modulus/high-strength fibers. The 1939 and 1962 resins are both claimed to be damage tolerant epoxies.

These prepregs were fabricated into 16-ply panels with quasi-isotropic lay-up configuration, $(0,+45,-45,90)_{S2}$. Each material was cured with a hot press according to the supplier's recommendations. The T300/934 ranged in thickness from 1.76 mm to 180 mm, the T650/1939 from 1.82 mm to 1.92 mm, the T650/1962 between 1.92 mm and 2.00 mm, the IM7/1939 was between 2.28 and 2.32 mm thick, and the IM7/1962 had a thickness ranging from 1.96 to 2.04 mm.

Specimens 10.16 $cm^2$ were machined from the composite panels for impact testing.

## 2. Impact Testing

The specimens were impacted using a Dynatup model 8200 drop weight apparatus. The data was obtained with a Dynatup 730 Data Acquisition System. The impactor had a mass of 1.77 kg with a 1.27-cm diameter hemispherical tup. The specimens were held tightly between two aluminum plates by a pneumatic clamping mechanism. The plates had holes 7.62 cm in diameter within which the composite panel was exposed. The specimens were all impacted at their centers.

## 3. Visual Damage

For each level of impact energy on each type of specimen, the visual damage to both sides of the panel was recorded and photographed.

## 4. Specimen Cross-Sectioning

For each impact energy level on each type of specimen, a cross-sectional cut was made perpendicular to the outer fibers and through the point of impact with a Buehler diamond wafering blade. The specimens were then examined and photographed by a Zeiss stereo-optical microscope at magnifications between 8 x and 20 x. Several of the IM7/1939 specimens were cross-sectionally cut parallel to the outer fibers and through the front surface crack. These specimens were photographed at magnifications between 8 x and 50 x.

# III. RESULTS AND DISCUSSION

## 1. Force-Time Plots From Impact Tests

The force-time plots, generated by the data acquisition system, of each specimen damaged from a drop height which induced fiber breakage showed a sharp drop in force at the maximum recorded load.

For impact tests which produced no fiber breakage there was no sharp drop in force, but rather a gradual reduction. Force-time plots for each drop height used on each material are presented in appendix A.

## 2. Absorbed Energy-Time Plots From Impact Tests

The smooth curves included on the force-time plots in appendix A are absorbed energy-time plots. A constant percentage of initial impact energy was lost during the impact of all of the materials tested, until the point of fiber breakage where the the output listed virtually 100 percent of the impact energy being absorbed. It must not be interpreted that all of the energy loss was released as damage to the impacted specimen. It has been found that vibrational waves most likely account for a substantial percentage of the lost impact energy (Ref. 4).

## 3. Maximum Force Versus Impact Energy Plots

Maximum force of impact values were plotted against their corresponding impact energy levels for each material. These results are given in figures 1 through 5. The individual plot for each material shows a somewhat linear correlation between the maximum force and the increasing impact energy until the critical impact energy level at which point the maximum force drops slightly and then levels out. The critical impact energy level is the impact energy corresponding to the peak force from the force-energy plots and takes place just before fiber breakage occurs. From the comparison of the maximum force versus impact energy plots for all the materials (fig. 6) it can be seen that the plot actually loosely follows an inverse parabolic curve.

## 4. Visible Surface Damage

The visible surface damage was recorded after impact for each specimen. The following results are given for all five materials tested. In addition, several photographs of the damaged specimens are presented in appendix A. The apparent fabric pattern surface of the composites in the photographs was due to the imprint of the Teflon release cloth used during the curing of the specimens. In order to reveal hard-to-see damaged areas on the front and back sides of the specimen, a fiber optic light source was placed on the surface of the panel with light angled sharply across the impacted area. This method of illumination greatly enhanced the photographs as well as enabled the researcher to record minute surface damage earlier than might otherwise be detected.

The T300/934 plates displayed no damage until a small crack appeared on the back surface of the specimen at 4.1 J. With the next impact energy level of 5.0 J, the plate showed a significant dent on the front and a fairly large split on the back. Fiber breakage was first recorded within the front dent at 6.1 J. A hole was nearly punched through the specimen at 11.3 J.

The T650/1939 plates first displayed damage as a hairline crack along the back surface visible at 6.2 J, but a full split did not occur on the back side until 11.3 J. At an impact energy of 8.2 J, a dent appeared on the front surface. Fiber breakage was not observed within the dent until 15.2 J. The last impact, having an energy of 20.3 J, nearly punctured the specimen.

The T650/1962 plates allowed no visible damage until a crack occurred on the back surface at an impact of 7.1 J. A minor dent was produced with an impact of 9.1 J. Fiber breakage was not observed until 15.1 J of impact energy.

The IM7/1939 plates withstood damage until 6.1 J when a front surface dent and a rear surface crack occurred. At an impact of 8.2 J, a small crack appeared beside the impactor dent on the front surface of the specimen. The crack was perpendicular to the direction of the outer layer of fibers. At 10.2 J, these perpendicular surface cracks were noticed on either side of the impactor dent. The perpendicular cracks were found on the front surface of all specimens impacted with energies above 8.2 J. In all cases, the cracks were from 3 mm to 8 mm in length. Larger dents with fiber breakage occurred at the 15.3 J energy level.

The IM7/1962 plates showed no damage until a hairline crack appeared on the back surface and a minor dent appeared on the impacted side at the 7.0 J energy level. The damage on the back surface fluctuated between a hairline crack and several long cracks until the impact energy of 17.2 J when the surface split and raised. A barely visible dent was noticed at the 12.2 J energy level. At 19.1 J, minor fiber breakage occurred in the front surface dent.

## 5. Cross-Sectional Visual Damage

A cross-sectional cut was made perpendicular to the outer fibers for each plate and the specimens were examined and photographed. Photographs of each material impacted at each energy level are presented in appendix A.

The T300/934 showed damage on the first impact which had an energy of 1.0 J. Minor delaminations and a small matrix crack were noticed at this energy level. An impact of 4.1 J produced a slight ridge on the back side of the specimen due to the great level of delaminations and matrix cracking. Fiber breakage occurred at the 6.0 J energy level. Impact energies of 7.1 J and above rapidly increased the amount of destruction towards a puncture hole.

The T650/1939 displayed several minor delaminations at an impact of 5.1 J. The next energy level of 6.2 J produced no damage. At the next impact energy level of 7.1 J, many delminations and much matrix cracking occurred. Fiber breakage was not noticed until 12.8 J.

The T650/1962 withstood damage until 7.1 J when a hairline delamination occurred. There were no noticeable cracks until the 12.2 J impact. At 15.0 J fiber breakage occurred within the specimen.

The IM7/1939 showed no damage until the 6.1 J impact which caused delmination. Matrix cracking was first recorded at 8.2 J. Fiber breakage first occurred at the 14.4 J energy level. The impact of highest force, 19.4 J, produced a near hole in the composite material. For some of the IM7/1939 specimens, a cross-sectional cut was made through the small surface crack on the front surface. For all of the impacts, the crack occurred only through the outer layer and perpendicular to the fiber direction in this layer. Under magnification it was clear that, at the site of the crack, the outer fibers were completely broken. For the more forceful impacts, deliminations were noticed under the topmost layer in the cracked region. Several cross-sectional photographs of these cracks are provided in appendix B.

The IM7/1962 displayed hairline delaminations on the first impact which had an energy of 4.0 J. Matrix cracking was first evident at 7.0 J. The damage from the impacts between the 8.2 J and 12.2 J energy levels were long delaminations with a few matrix cracks. Much matrix cracking was the result of the 16.1 J impact. At 18.3 J a small amount of fiber breakage occurred within the specimen. With regards to fiber breakage damage tolerance, the IM7/1962 performed superior to all the other materials. The IM7/1962 supported a force of almost 800 N more than the second most damage resistant material, T650/1962, before fiber breakage occurred.

## IV. CONCLUSION

This study was designated as an impirical presentation to benefit the designing engineer by showing the response of four damage tolerant composite systems to a blunt, low velocity impact.

Low velocity impact testing of composite panels can provide essential data on a fiber/resin system. Force-time plots of the impact event show the maximum force that the composite plate can support before fiber breakage occurs. Graphs of the maximum load versus impact energy show the critical energy level at which fiber breakage takes place and extensive tensile strength losses may occur. Surface photograhic documentation provides a means of identifying damage without the destructive evaluation of the material. Cross-sectional photography provides a detailed account of the damage modes a specimen undergoes due to impacts of varying energies.

The damage modes for all the specimens followed in the same order. Minor internal delaminations were the first damage to appear. Soon afterward, matrix cracking began within the specimen. A rear crack and then a front dent were the next damages to occur. The next damage level was fiber breakage within the specimen, followed by fiber breakage appearing within the front dent. Fiber breakage was next seen on the back surface of the panel, followed by a puncture hole.

The T300/934 was employed as a baseline material because of the large data base that exists for that fiber/resin system. The T300/934 supported a maximuum impact load of 2,367 N. The IM7/1939 upheld a force of 3,894 N, 65 percent greater than the maximum impact load capability of the T300/934. The T650/1939 supported a maximum load of 4,481 N, 89 percent greater than the maximum force of the T300/394. The T650/1962 held 5,408 N before breakage which was an increase of 129 percent over the T300/934. The IM7/1962 upheld a load of 6,203 N, a 162 percent improvement from the T300/934. The T300/934 had an impact energy of 9.1 at its maximum load. The IM7/1939's maximum load occurred at an impact of 11.2 J, the T650/1939 impact of 11.3 J provided its greatest load, the T650/1962 had an impact energy of 14.2 at its maximum force, and the IM7/1962's greatest load occurred at an impact energ of 17.5 J.

Throughout the study, the 1962 resin system proved to be more damage resistant than the 1939 resin system. The IM7/1962 prepreg had more superior impact damage resistance than the other three damage tolerant composite materials.

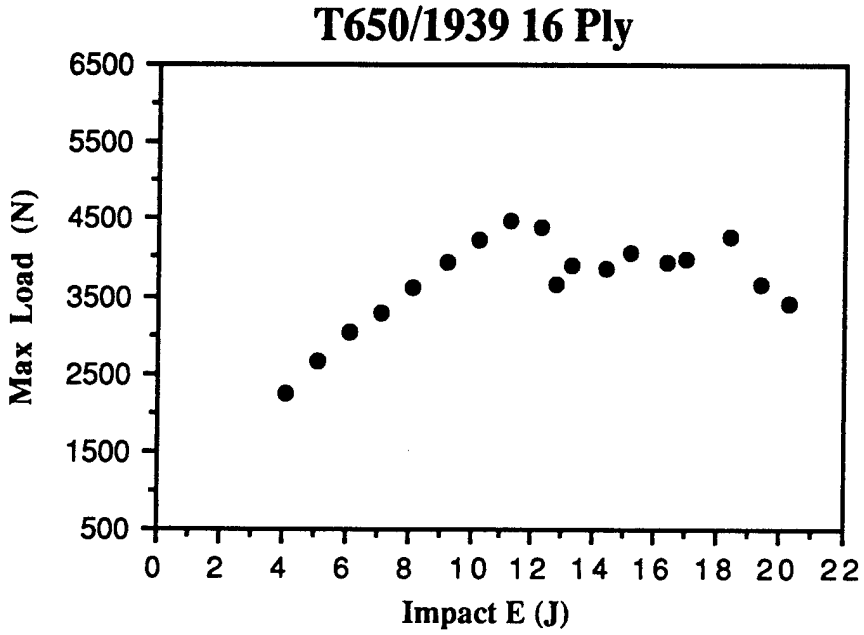


Figure 1. Maximum load versus impact energy for T650/1939.

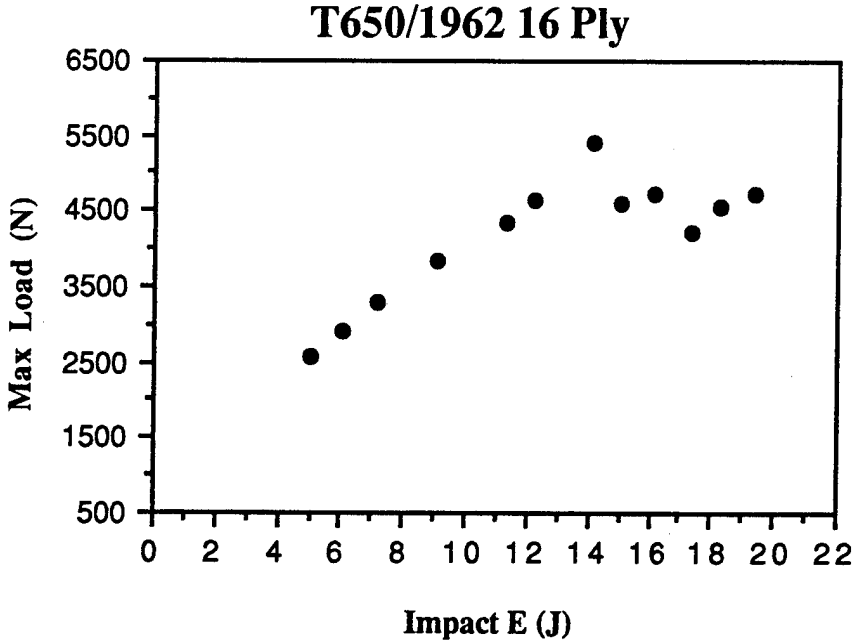


Figure 2. Maximum load versus impact energy for T650/1962.

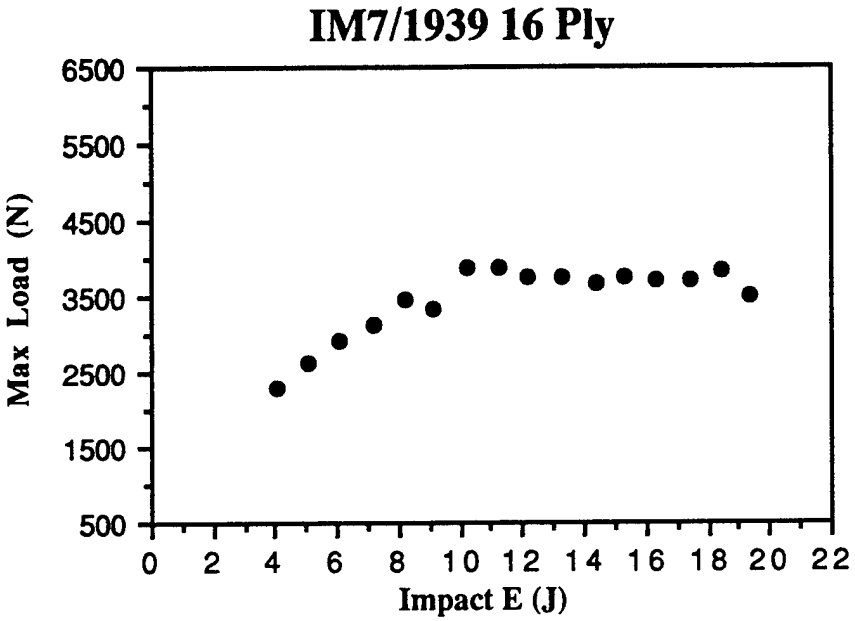


Figure 3. Maximum load versus impact energy for IM7/1939.

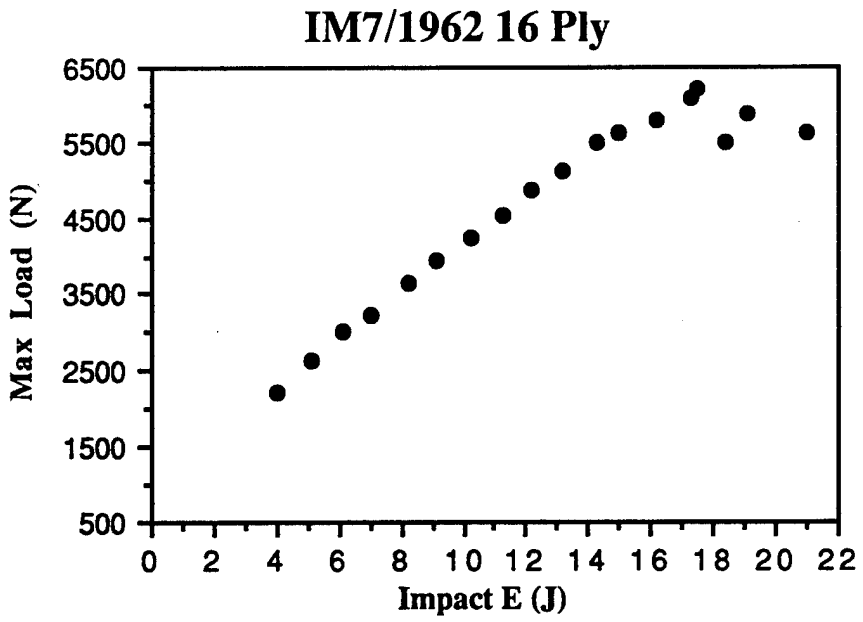


Figure 4. Maximum load versus impact energy for IM7/1962.

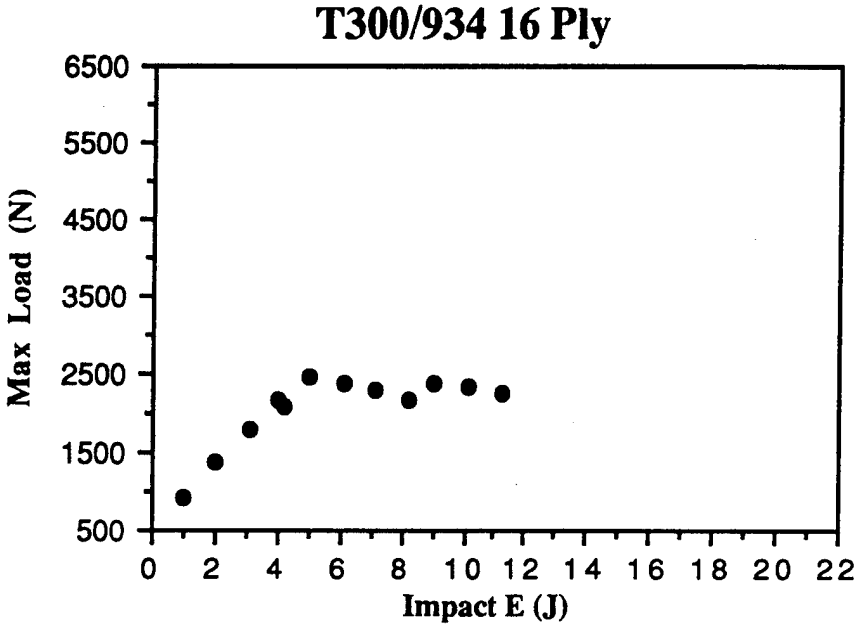


Figure 5. Maximum load versus impact energy for T300/934.

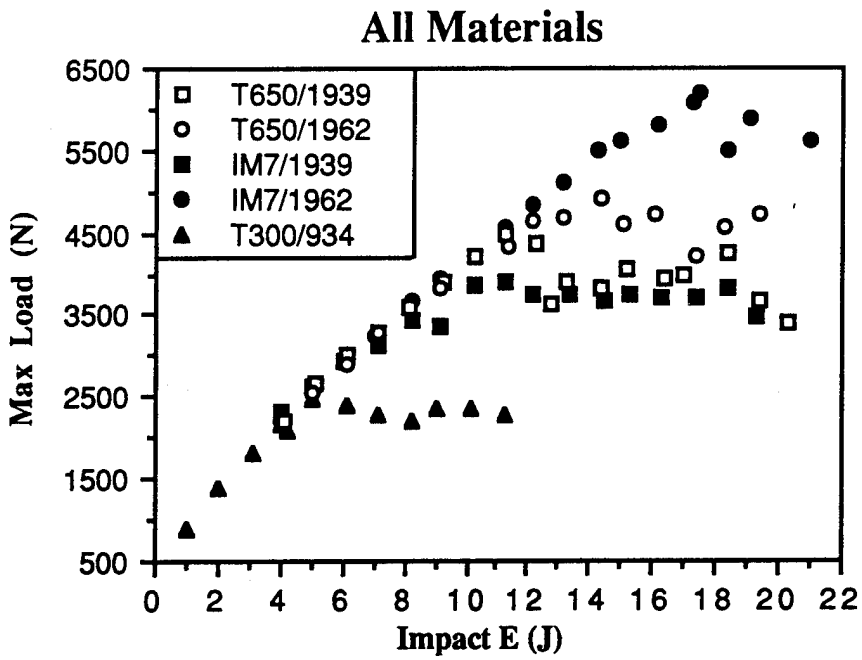


Figure 6. Maximum load versus impact energy for all materials.

# APPENDIX A

## Instrumented Output, Cross-Sectional Photographs and Surface Photographs of Each Material

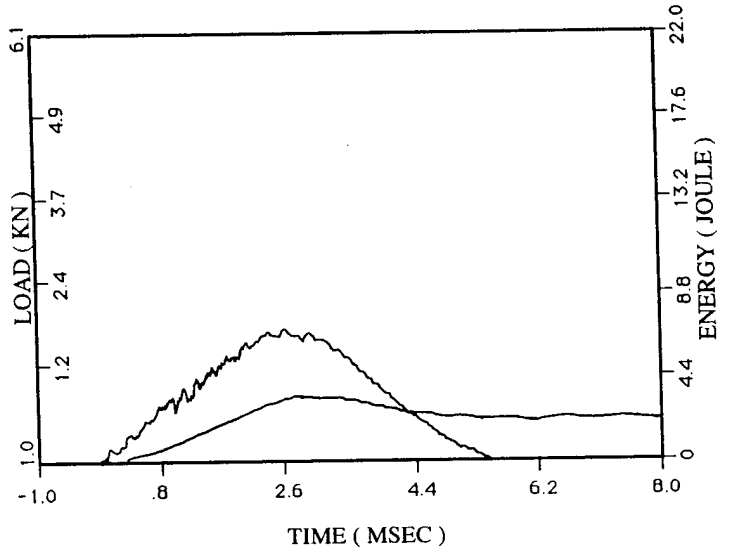


INSTRUMENTED OUTPUT

CROSS SECTION

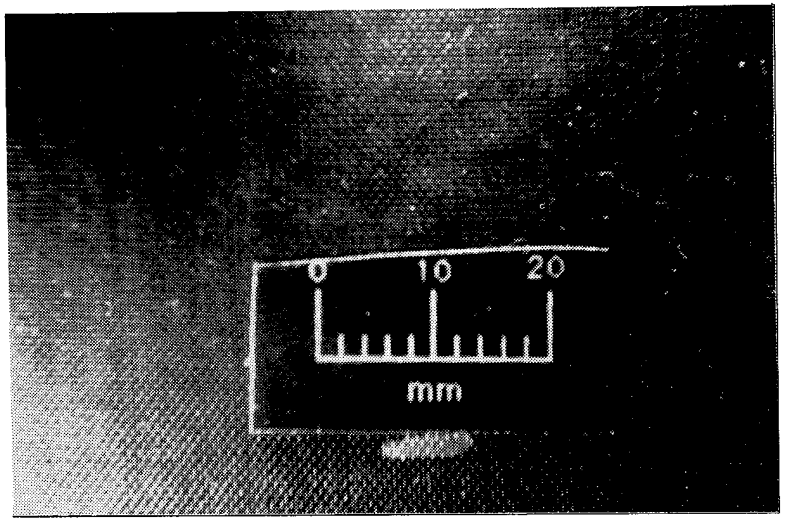


FRONT

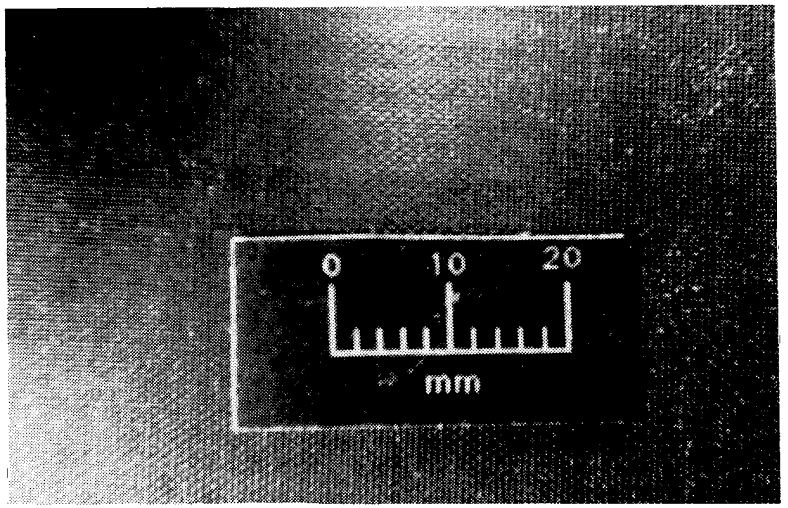


BACK

**T300/934 IMPACT ENERGY 3.1 J**

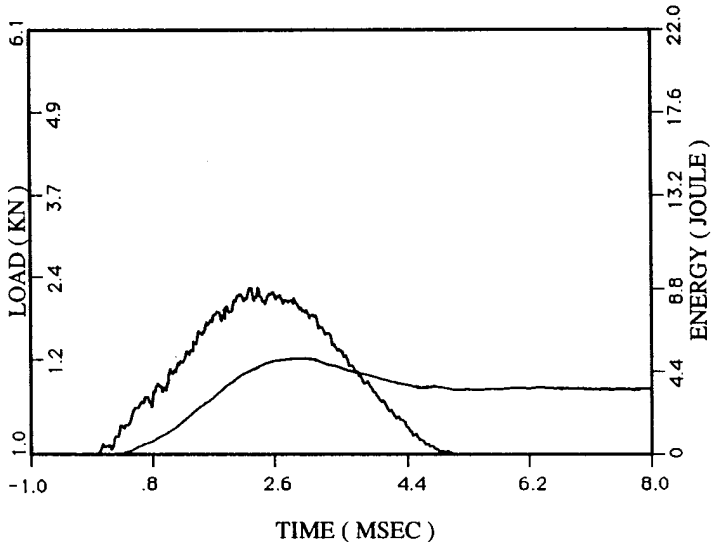


INSTRUMENTED OUTPUT

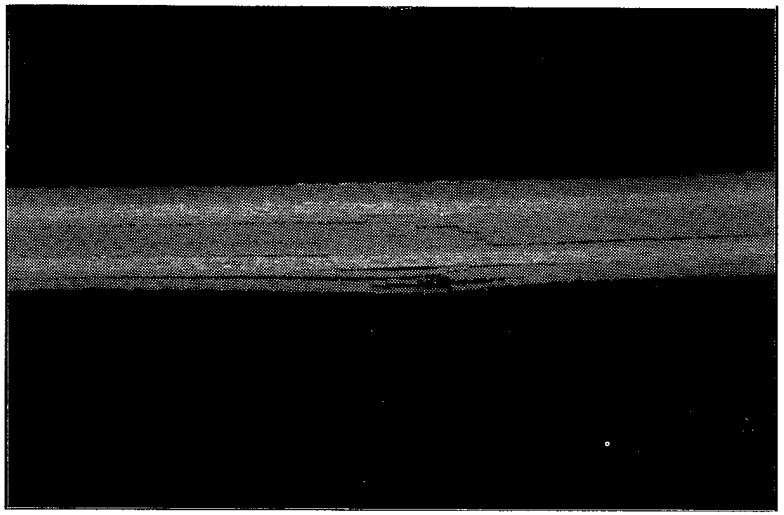

CROSS SECTION

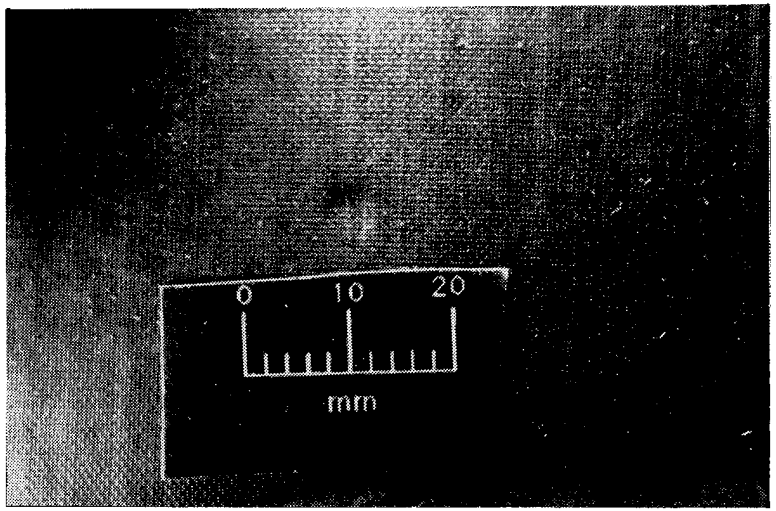


FRONT

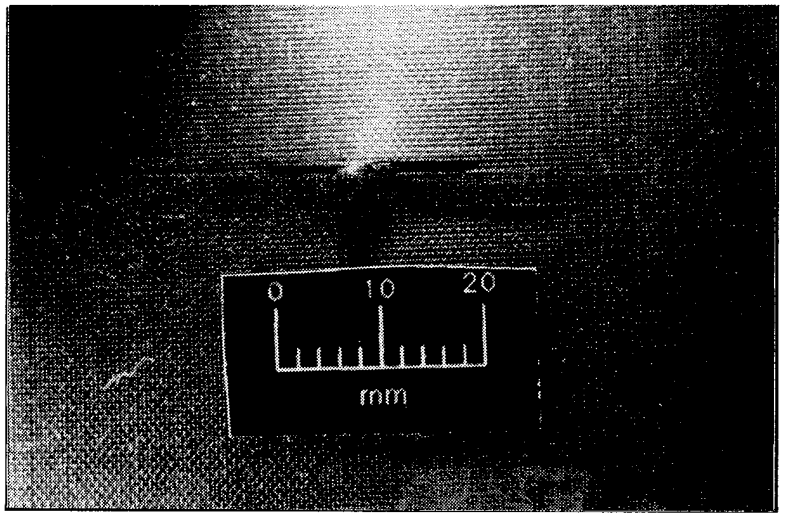


BACK

**T300/934 IMPACT ENERGY 5.0 J**

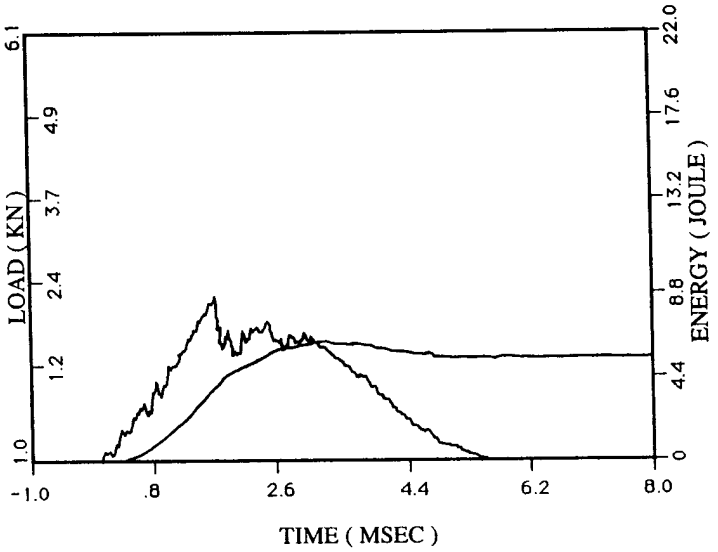


INSTRUMENTED OUTPUT

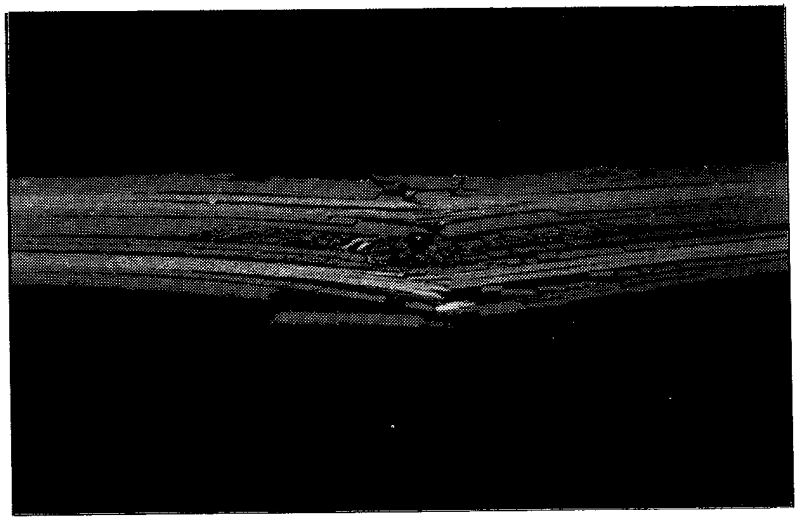

CROSS SECTION

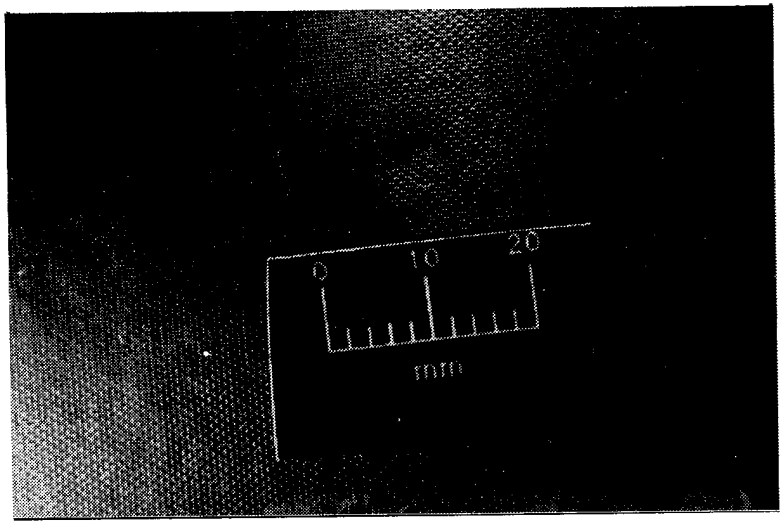


FRONT

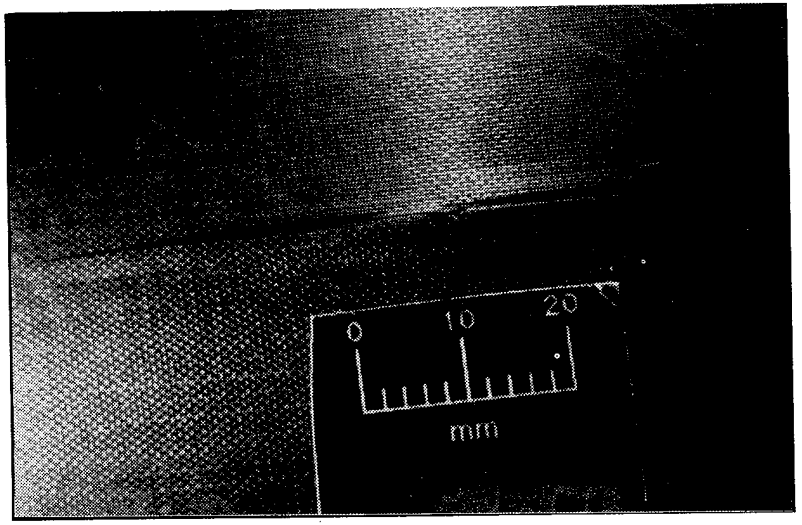


BACK

**T300/934 IMPACT ENERGY 6.1 J**

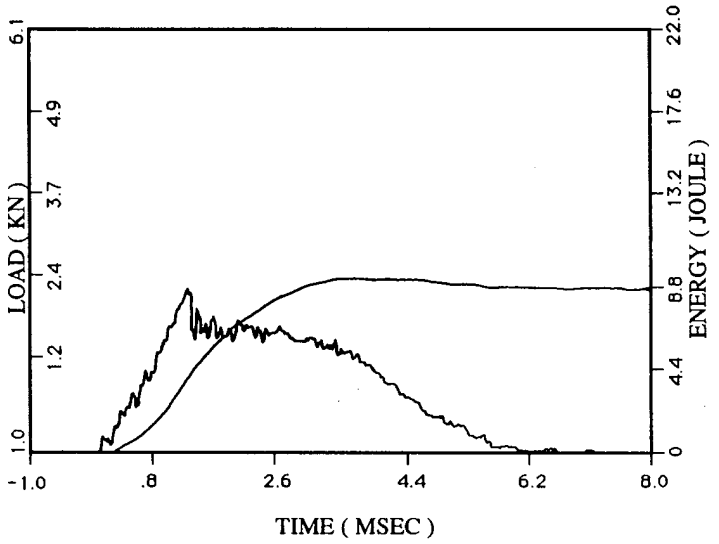


INSTRUMENTED OUTPUT

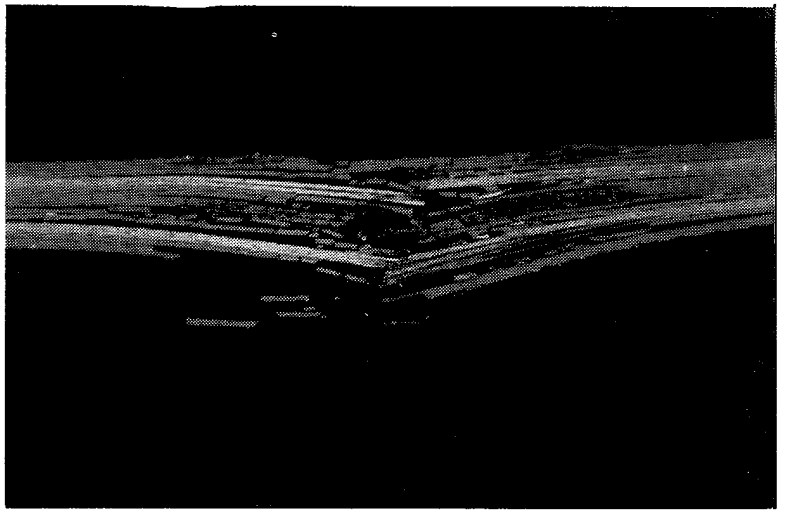

CROSS SECTION

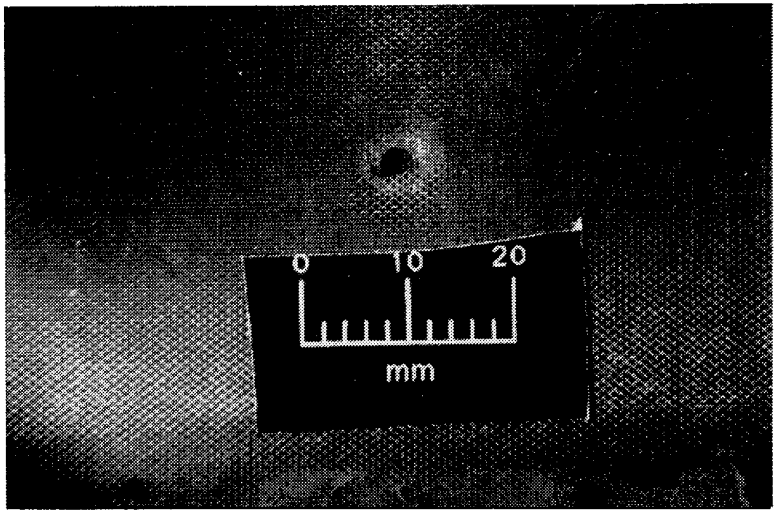


FRONT

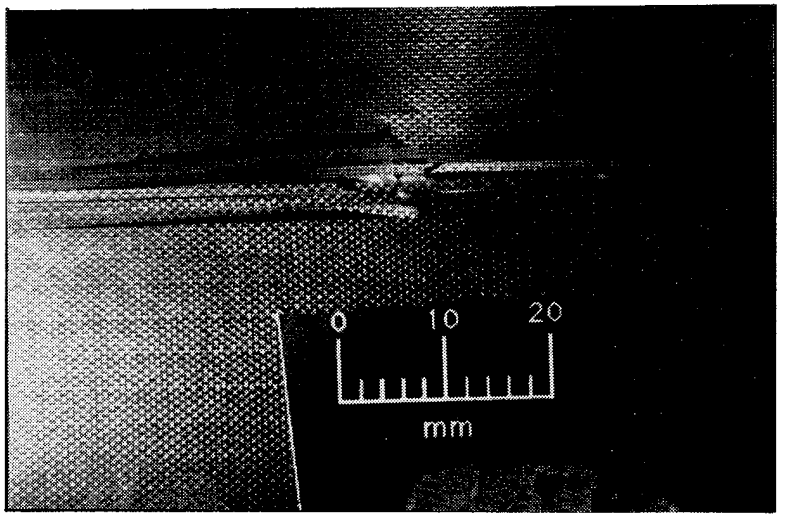


BACK

**T300/934 IMPACT ENERGY 9.1 J**

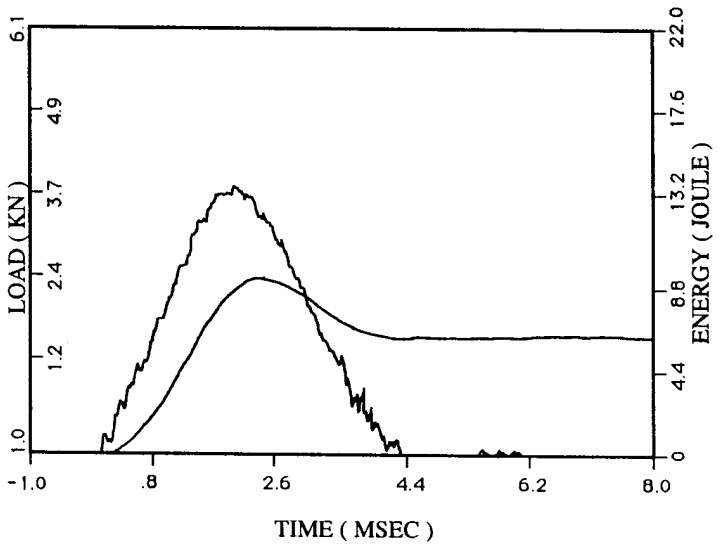


INSTRUMENTED OUTPUT

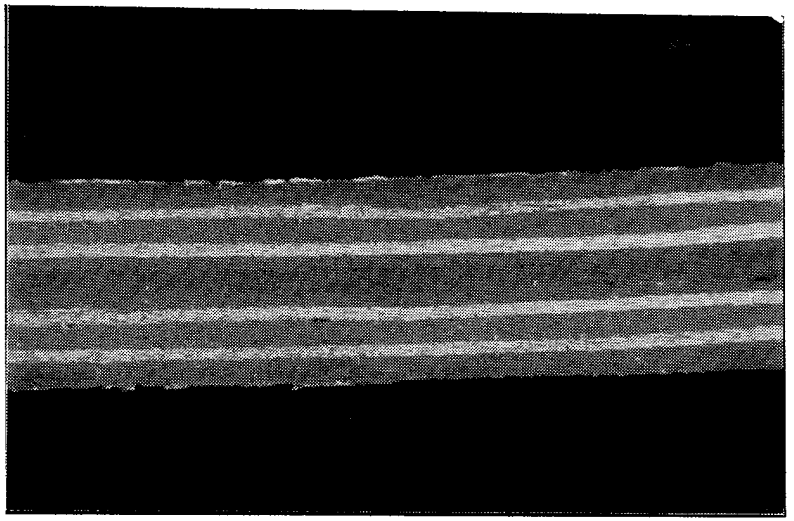

CROSS SECTION

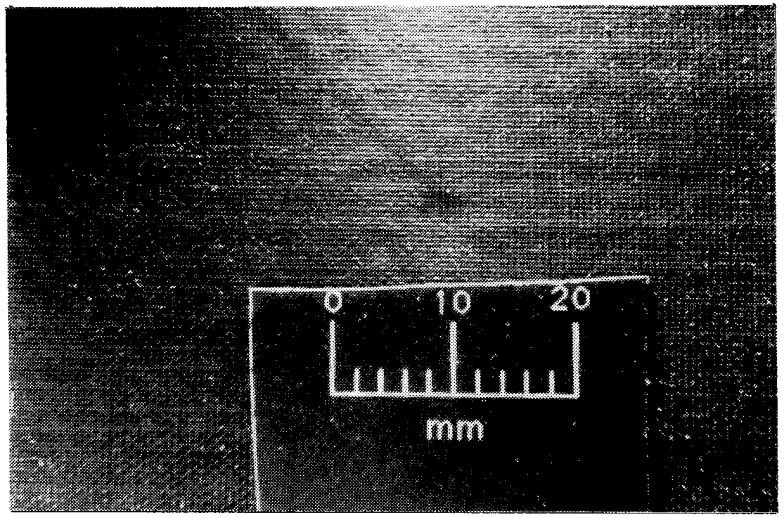


FRONT

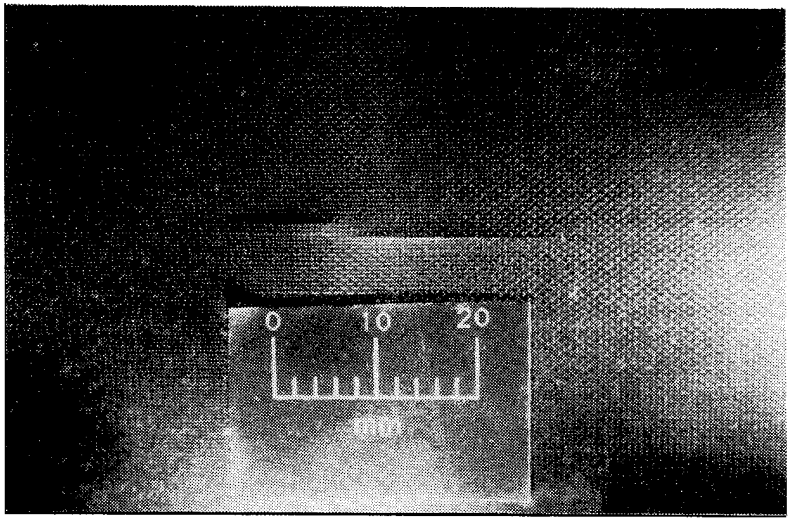


BACK

**T650/1939 IMPACT ENERGY 9.2 J**

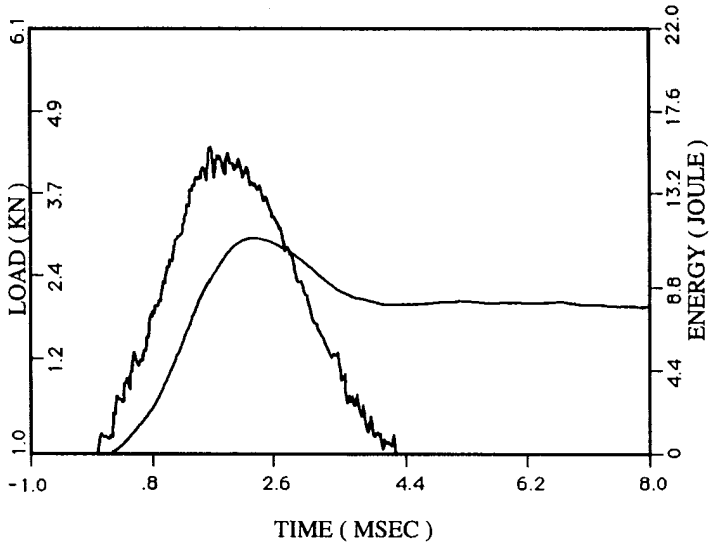


INSTRUMENTED OUTPUT

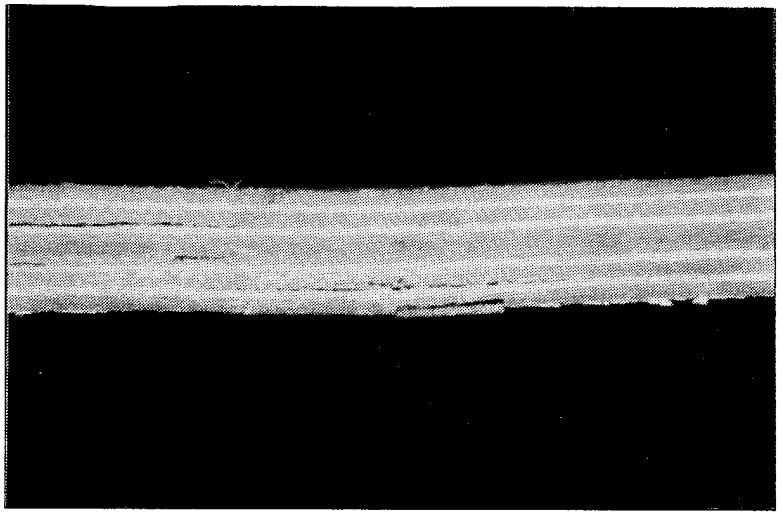

CROSS SECTION

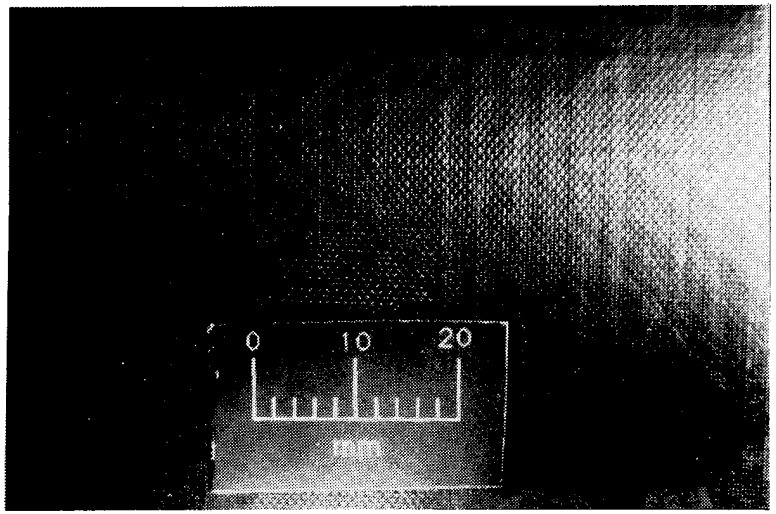


FRONT

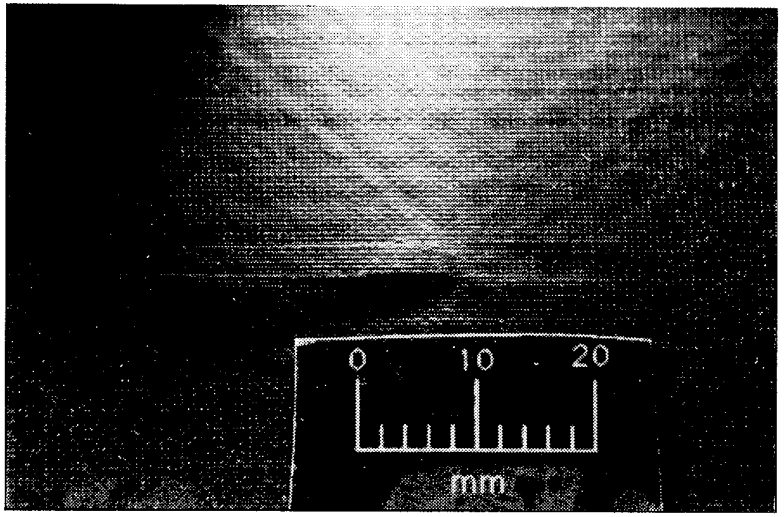


BACK

**T650/1939 IMPACT ENERGY 11.3 J**

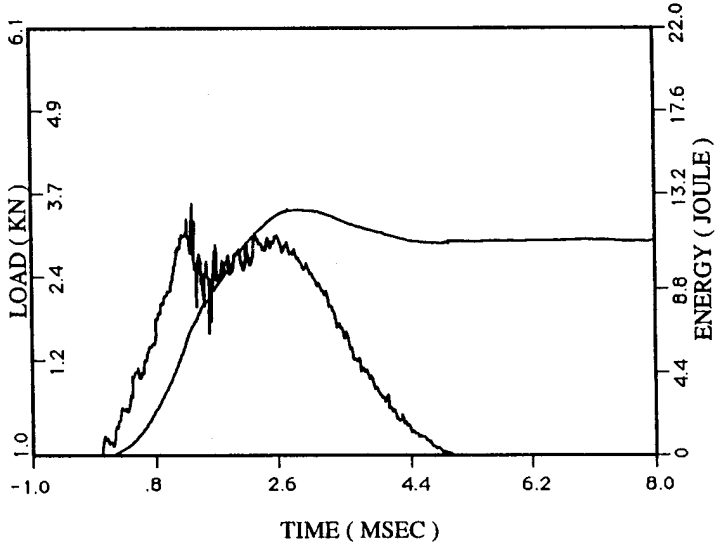


INSTRUMENTED OUTPUT

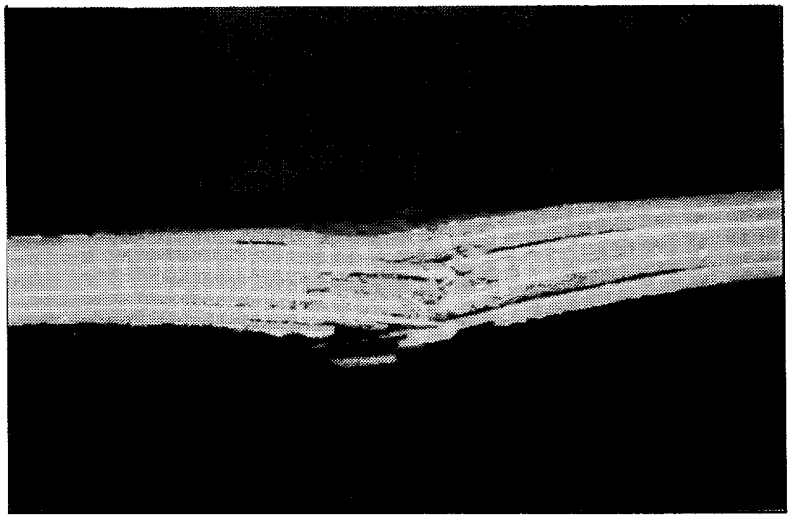

CROSS SECTION

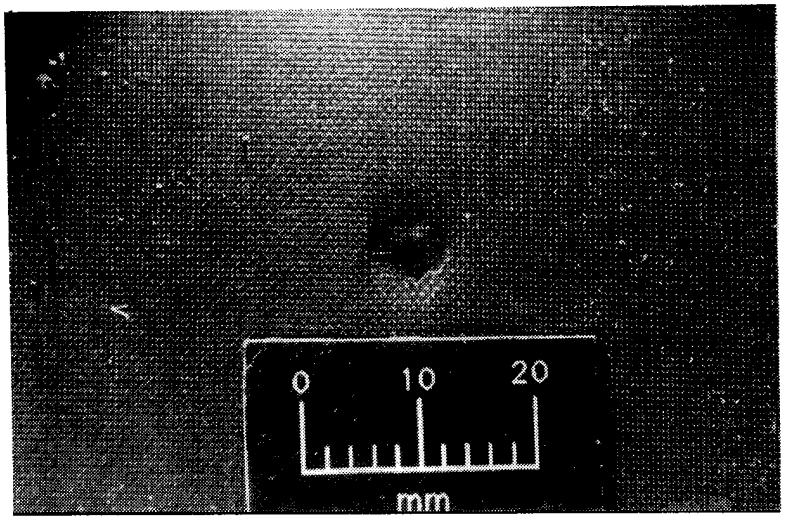


FRONT

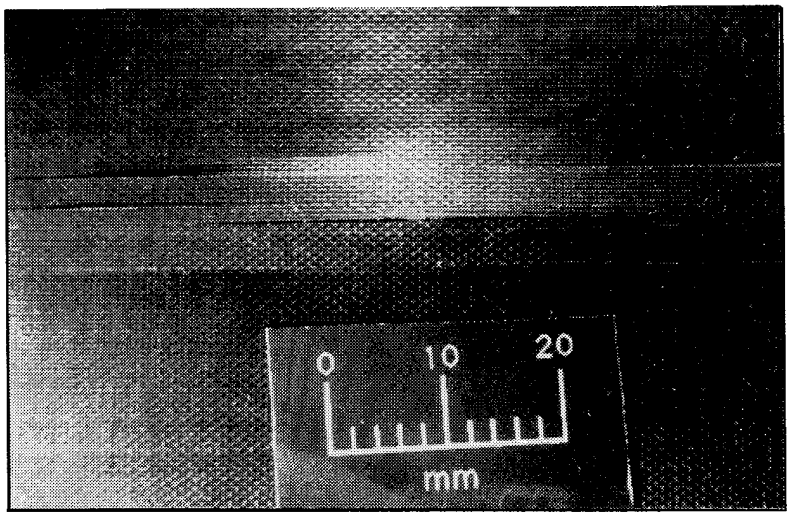


BACK

**T650/1939 IMPACT ENERGY 12.8 J**

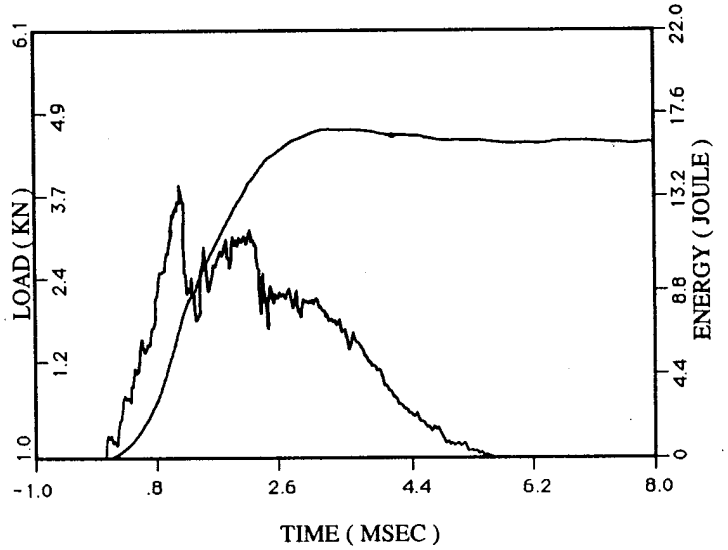


INSTRUMENTED OUTPUT

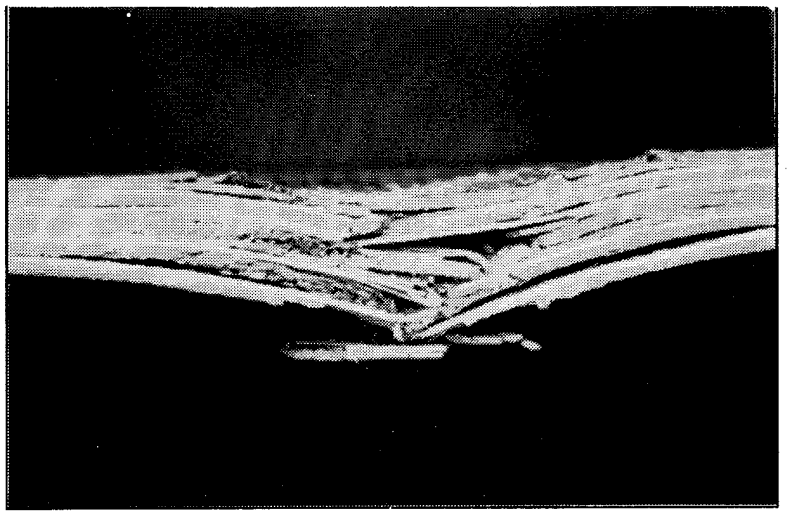

CROSS SECTION

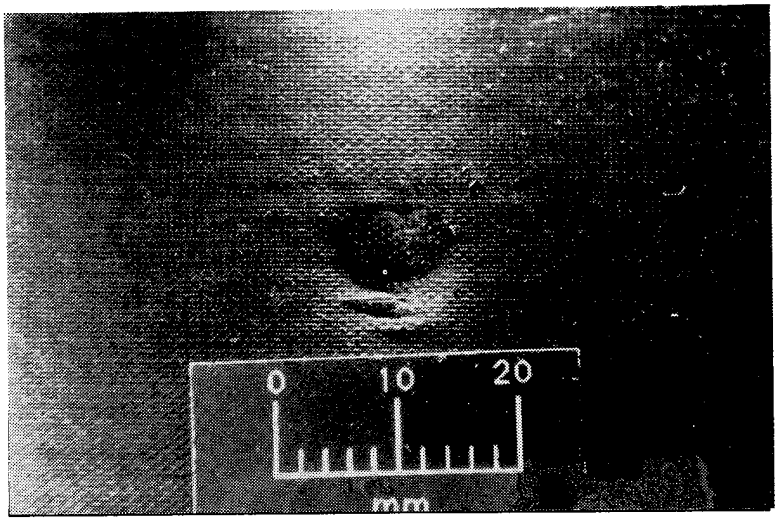


FRONT

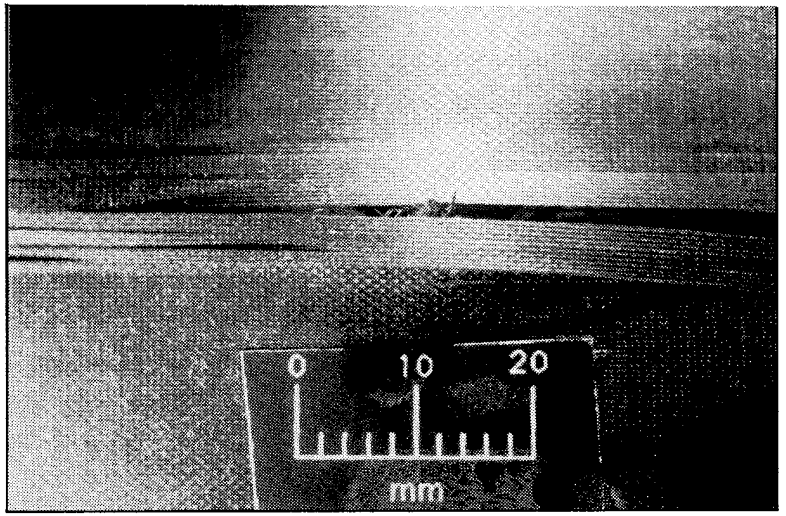


BACK

**T650/1939 IMPACT ENERGY 17.0 J**

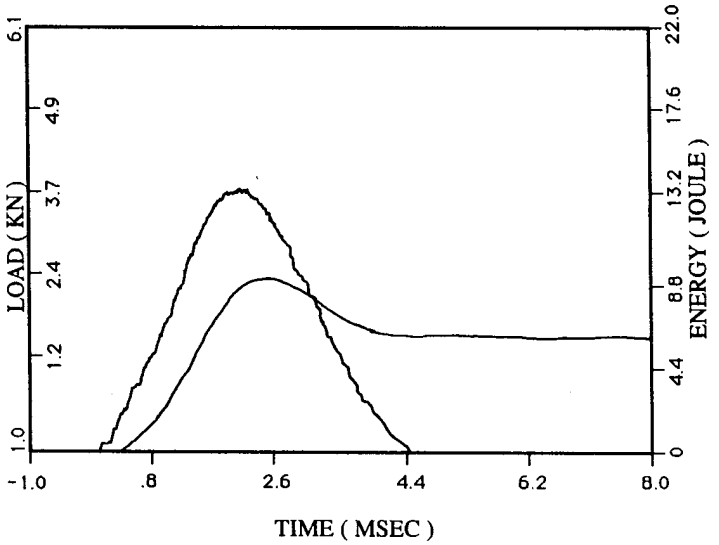


INSTRUMENTED OUTPUT

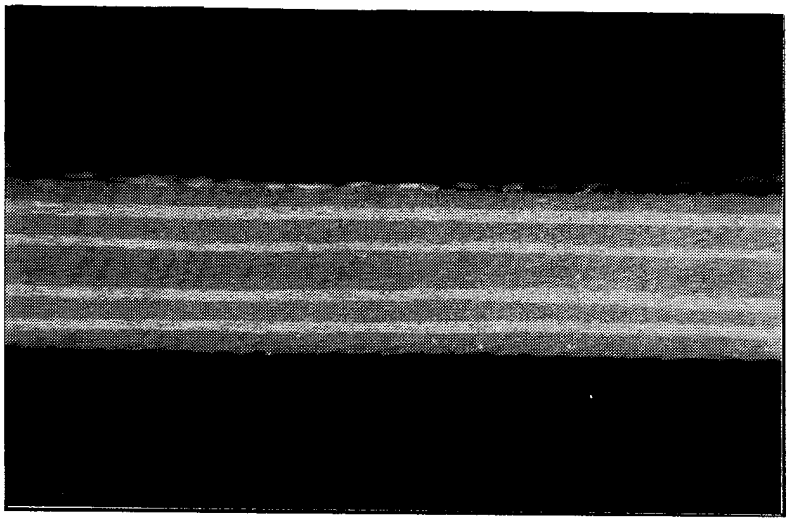

CROSS SECTION

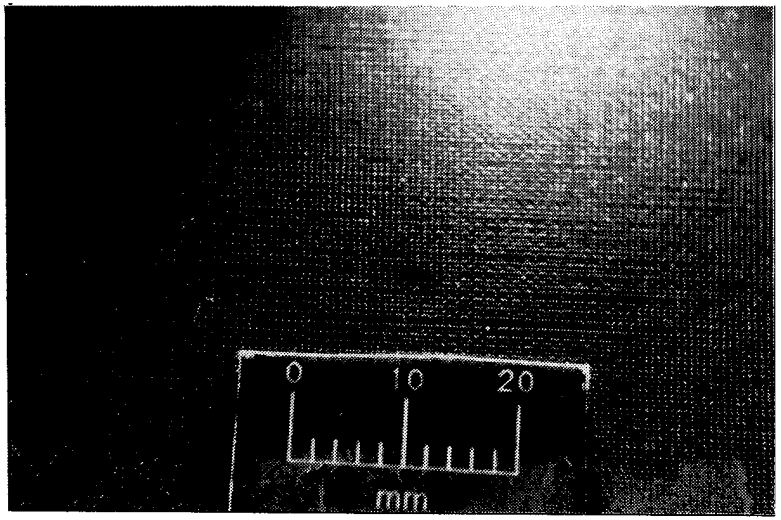


FRONT

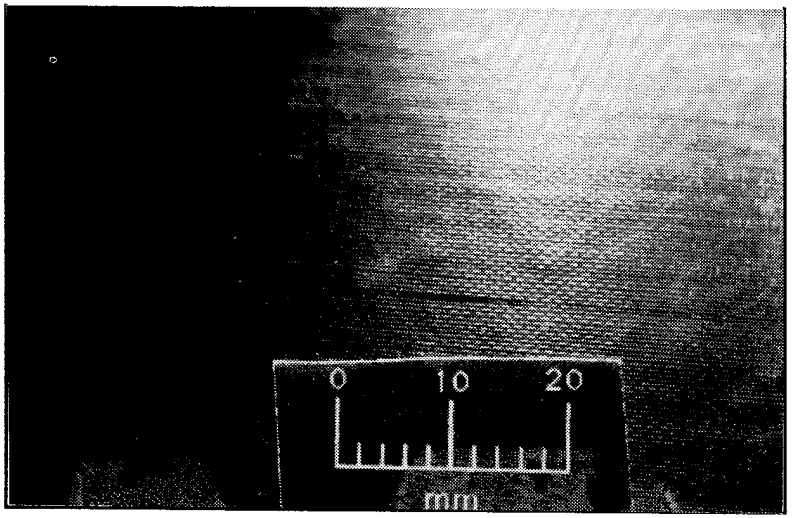


BACK

**T650/1962 IMPACT ENERGY 9.1 J**

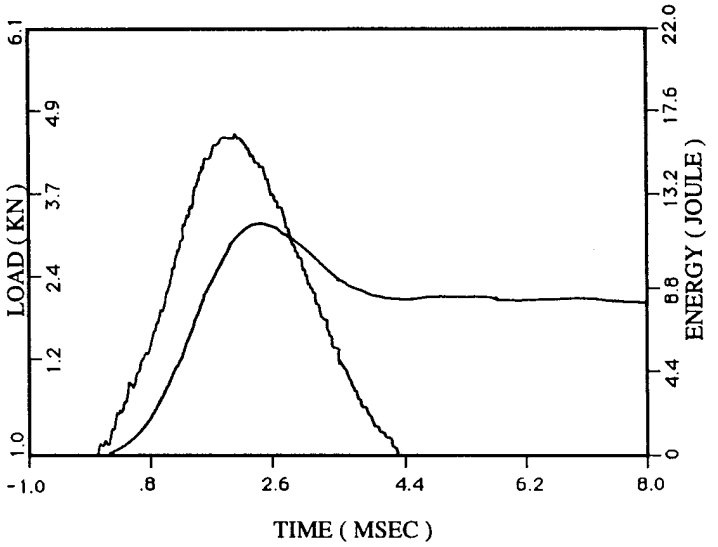


INSTRUMENTED OUTPUT

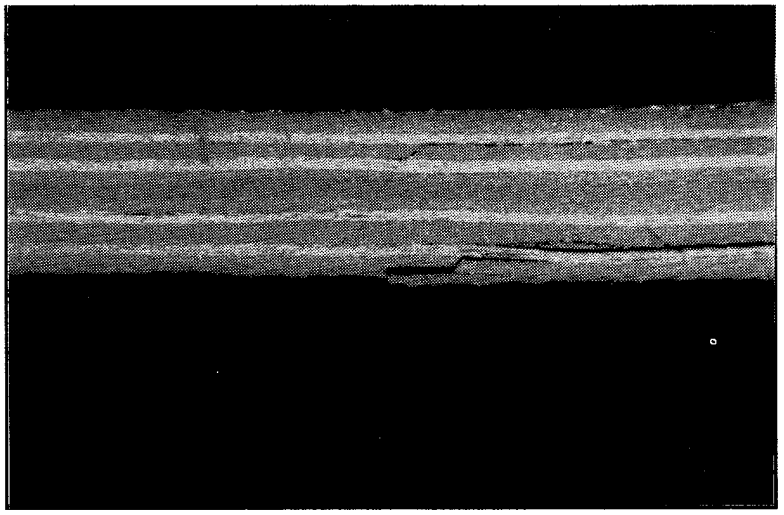

CROSS SECTION

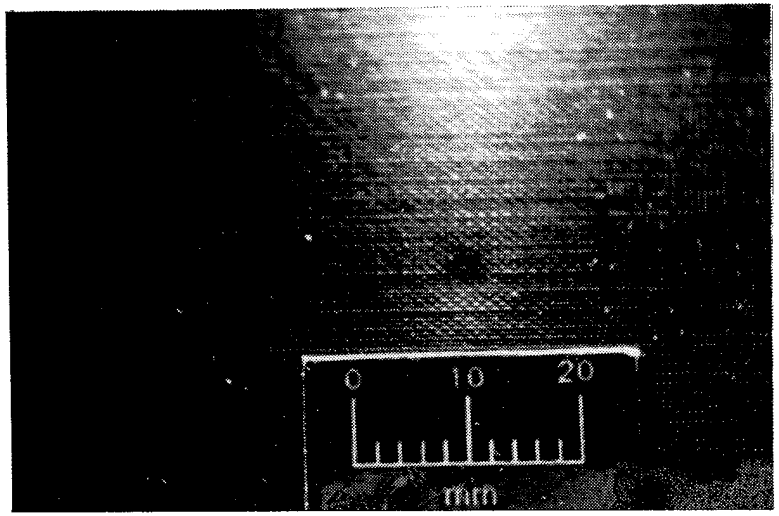


FRONT

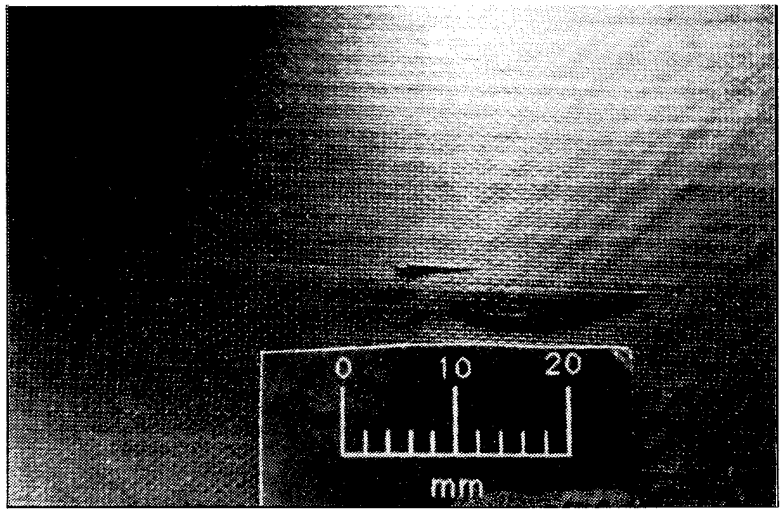


BACK

**T650/1962 IMPACT ENERGY 12.2 J**

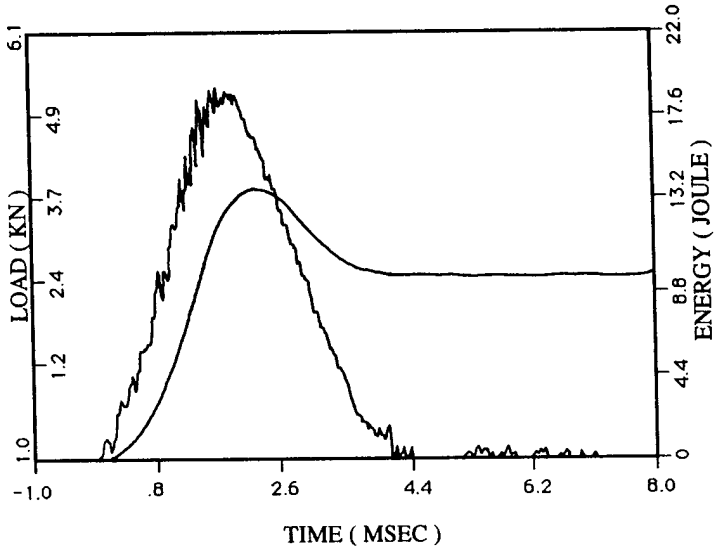


INSTRUMENTED OUTPUT

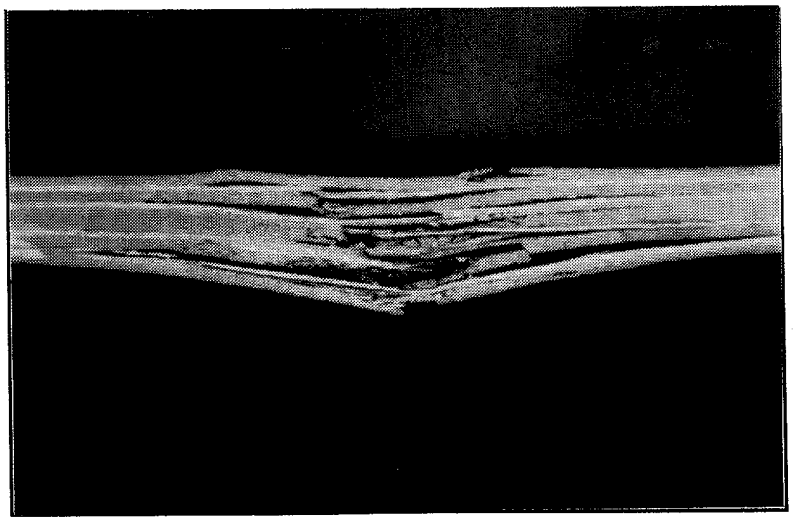

CROSS SECTION

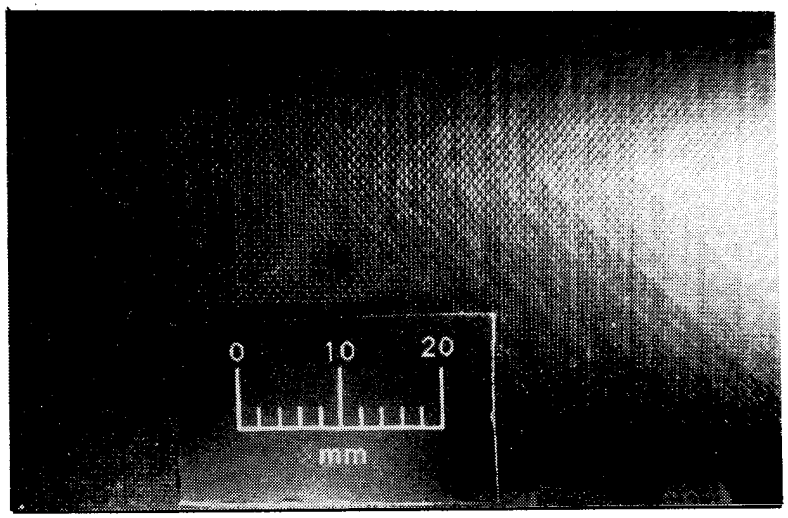


FRONT

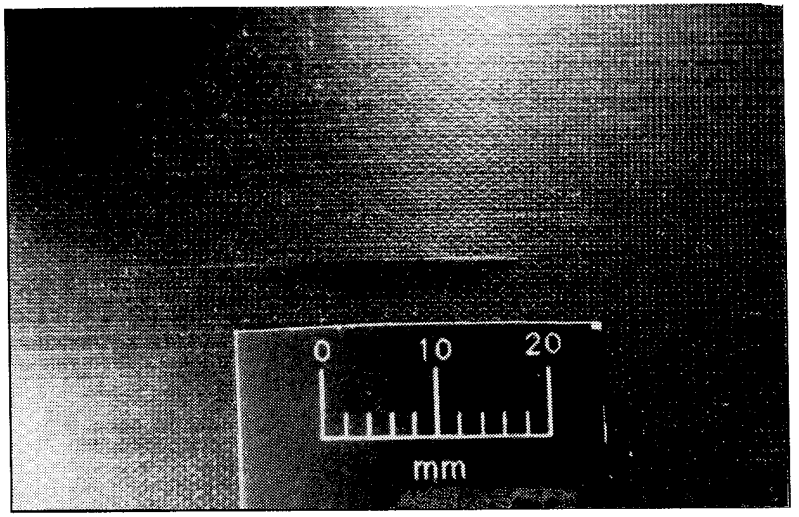


BACK

**T650/1962 IMPACT ENERGY 14.2 J**

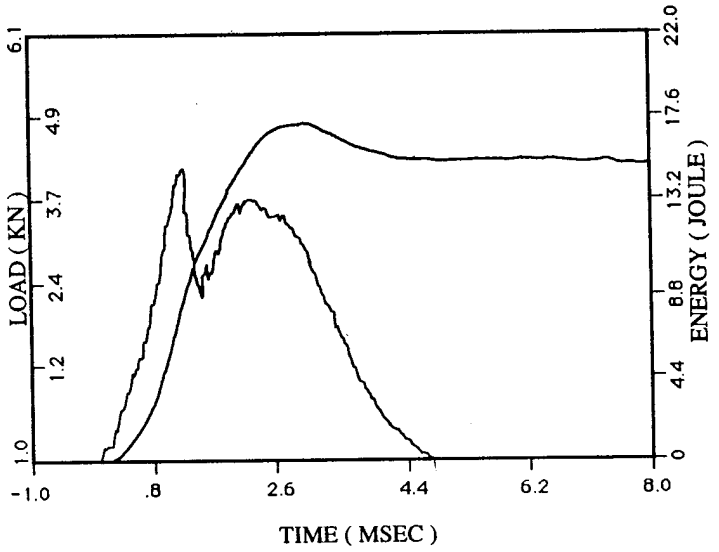


INSTRUMENTED OUTPUT

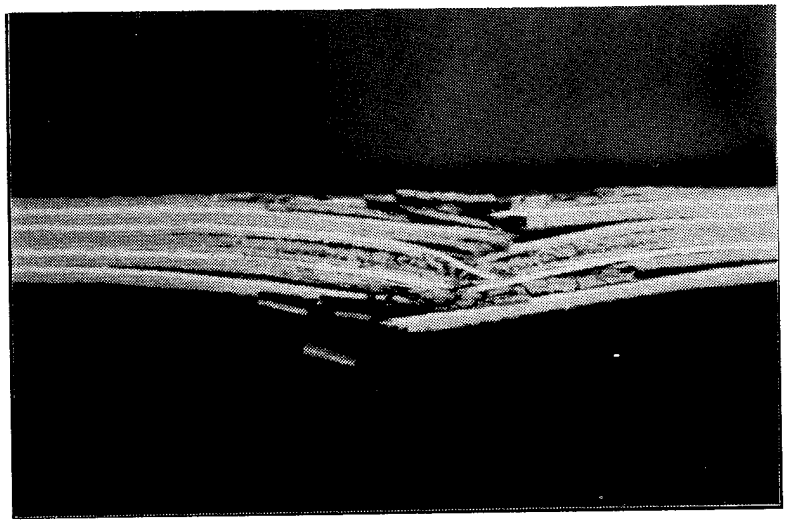

CROSS SECTION

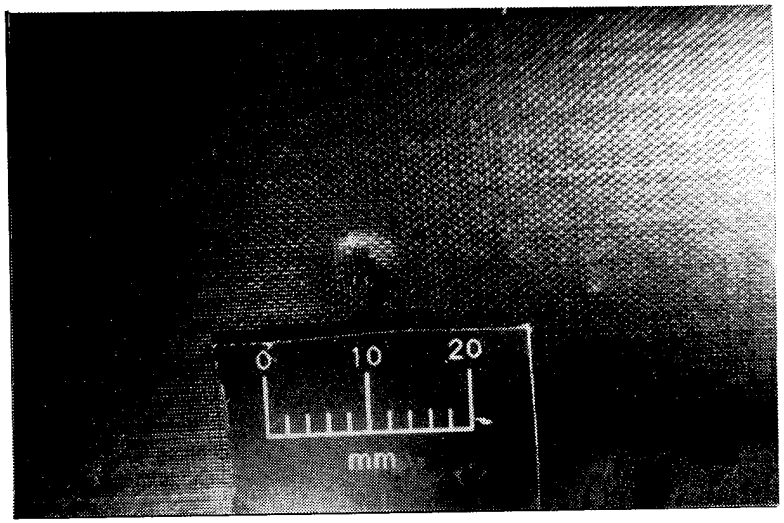


FRONT

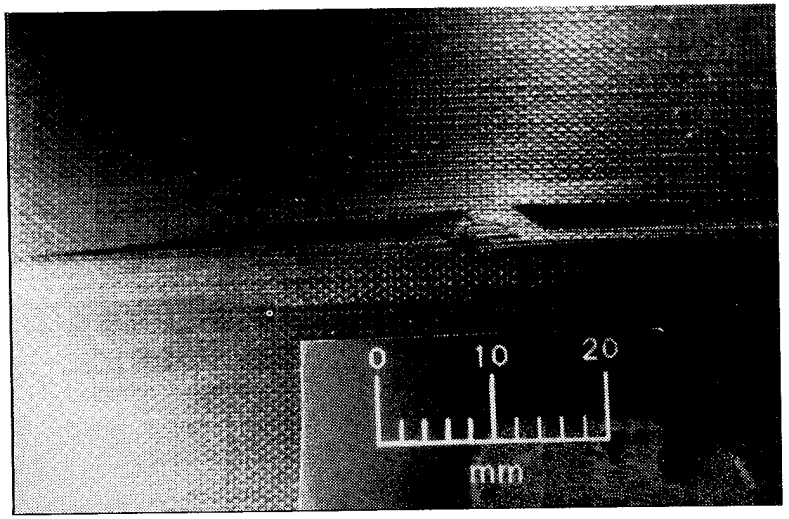


BACK

**T650/1962 IMPACT ENERGY 17.4 J**

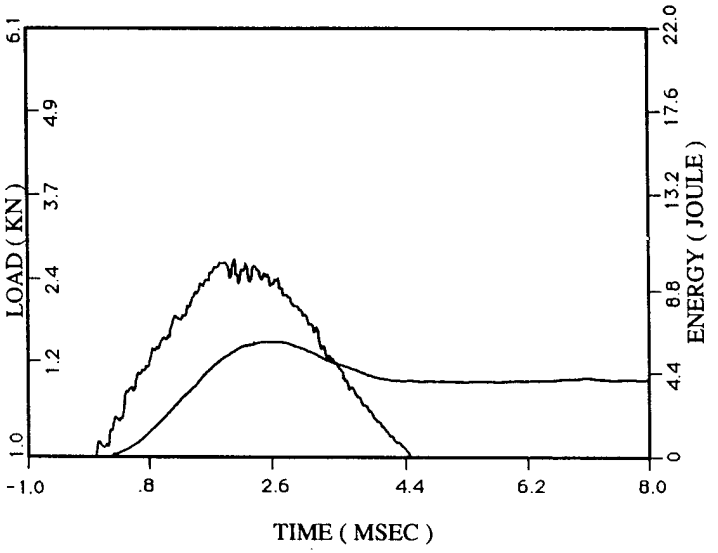


INSTRUMENTED OUTPUT

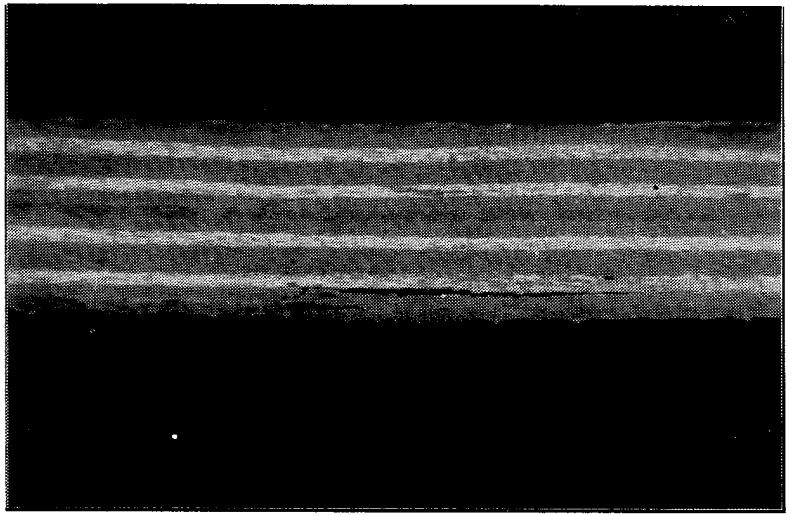

CROSS SECTION

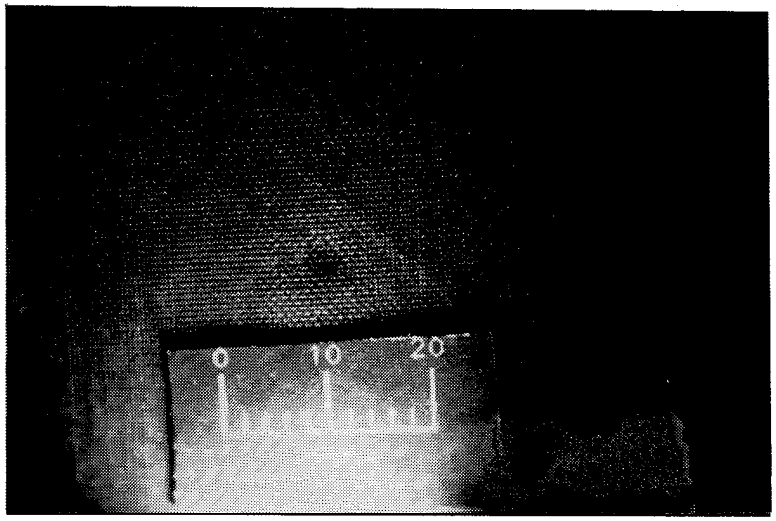


FRONT

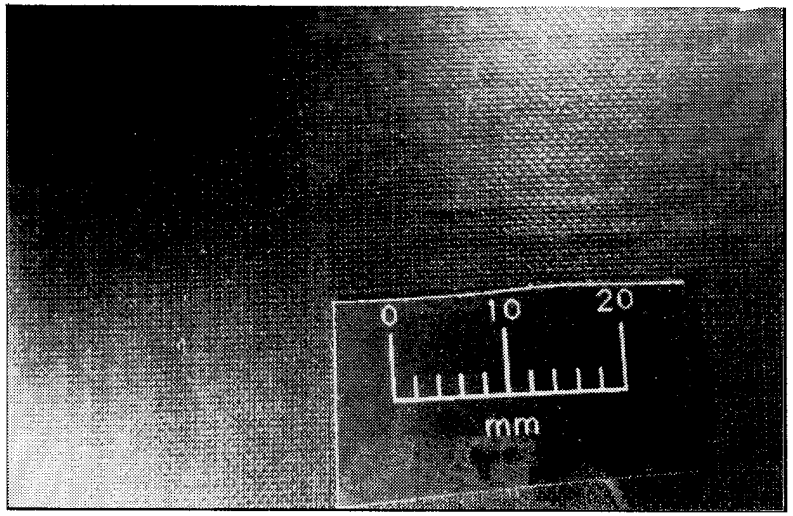


BACK

**IM7/1939 IMPACT ENERGY 6.1 J**

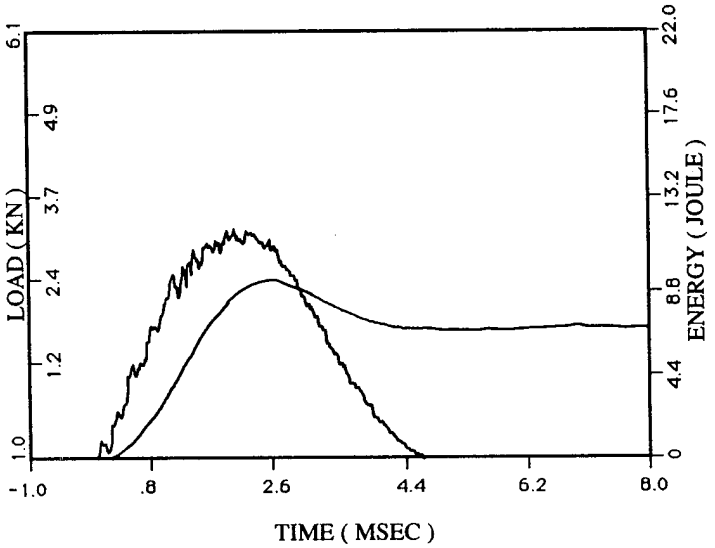


INSTRUMENTED OUTPUT

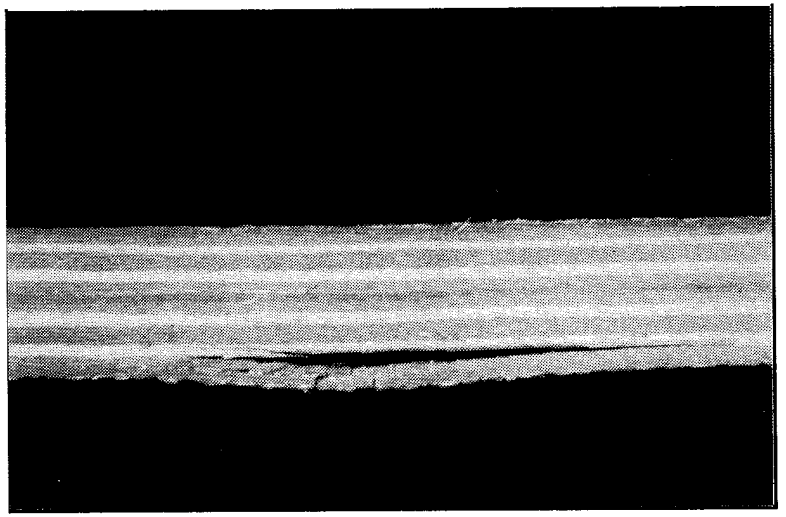

CROSS SECTION

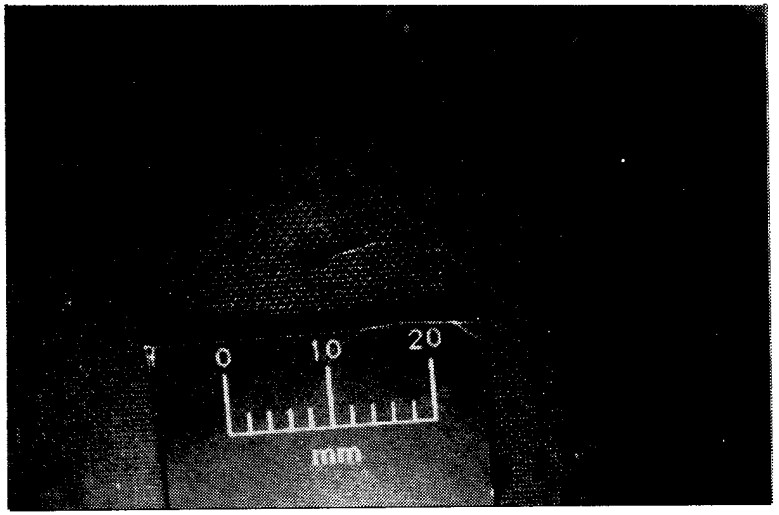


FRONT

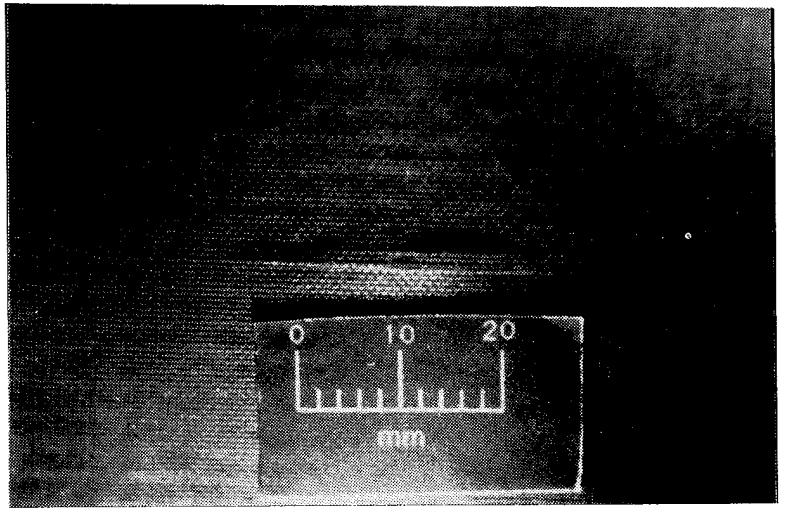


BACK

**IM7/1939 IMPACT ENERGY 9.2 J**

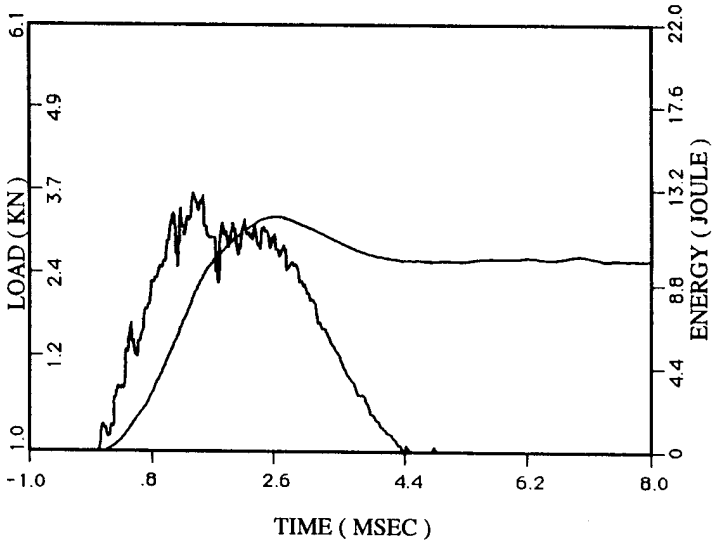


INSTRUMENTED OUTPUT

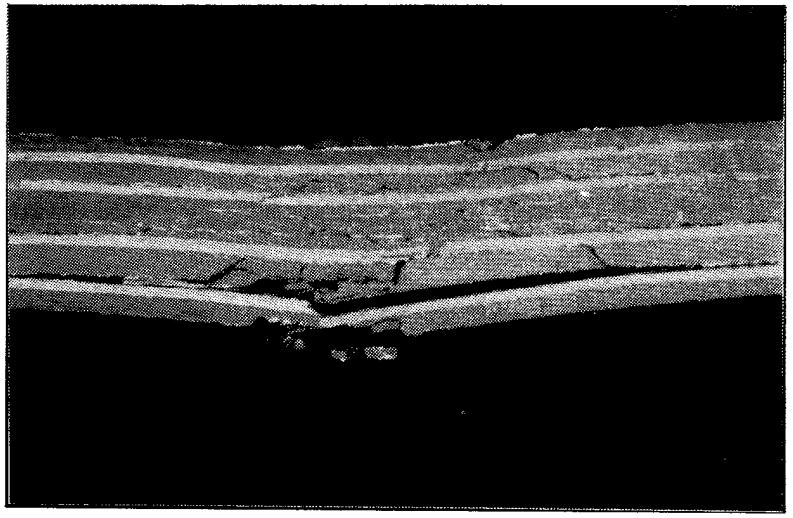

CROSS SECTION

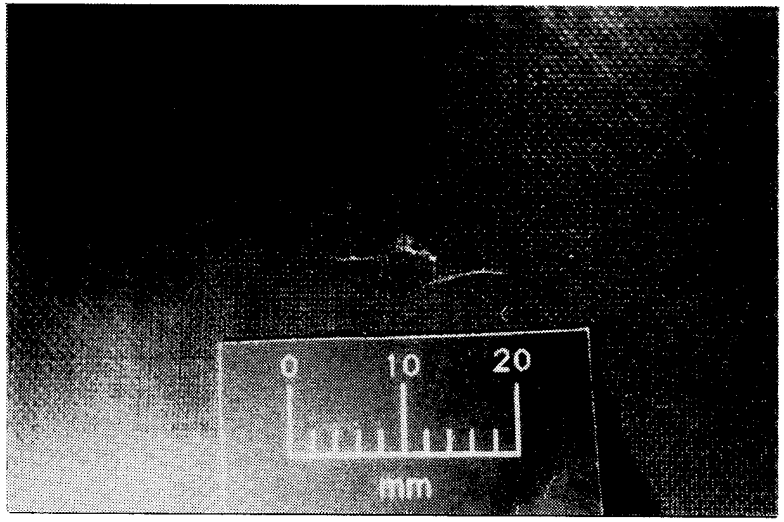


FRONT

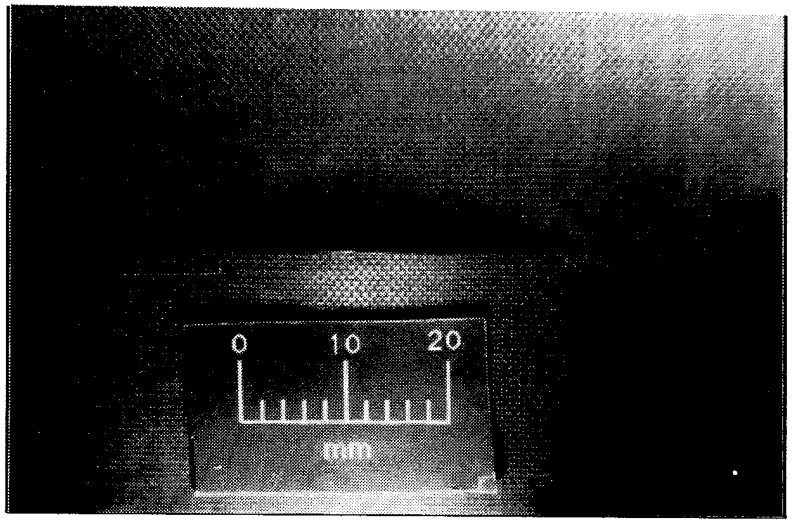


BACK

**IM7/1939 IMPACT ENERGY 12.2 J**

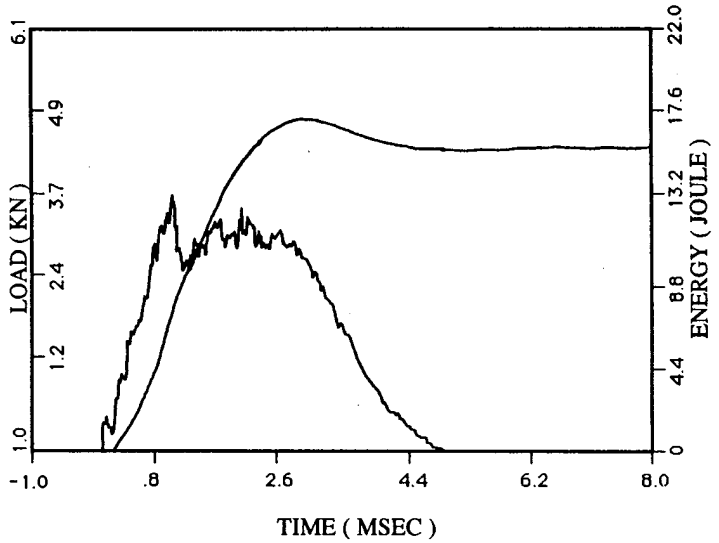


INSTRUMENTED OUTPUT

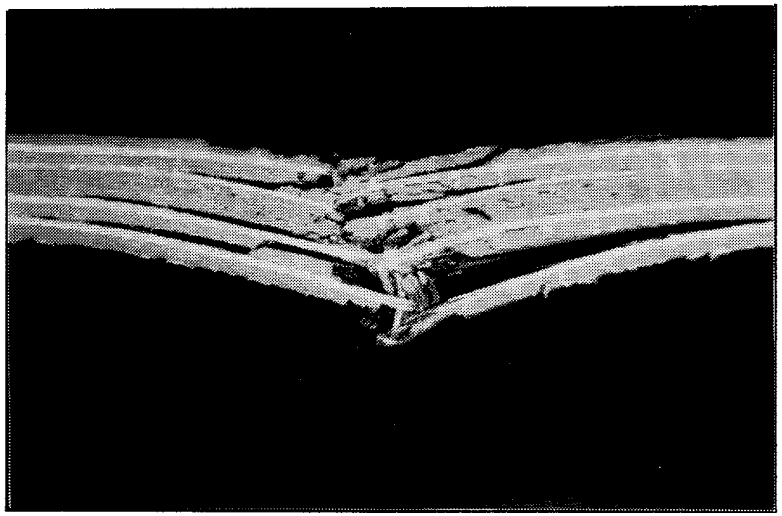

CROSS SECTION

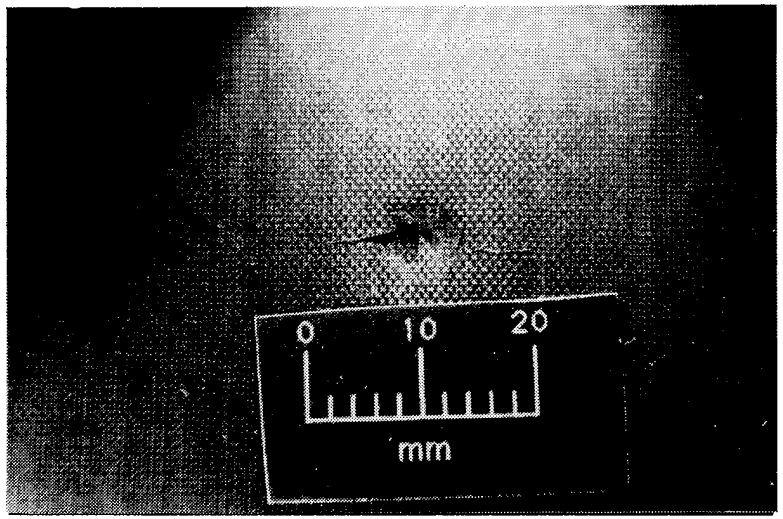


FRONT

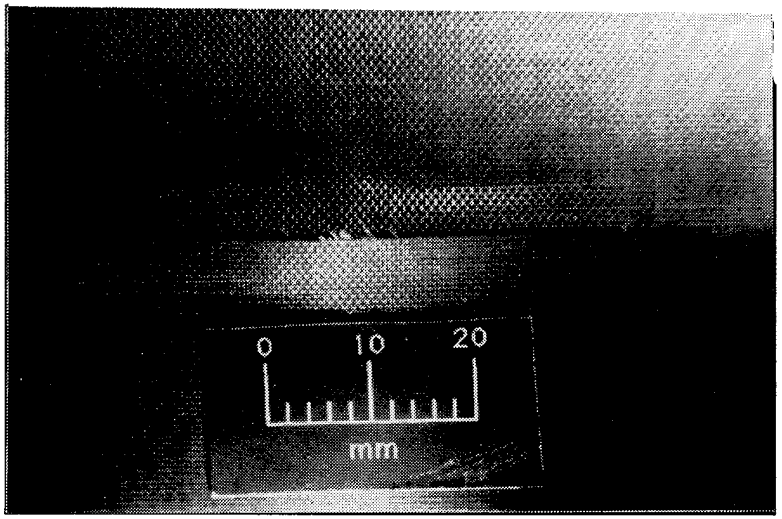


BACK

**IM7/1939 IMPACT ENERGY 17.4 J**

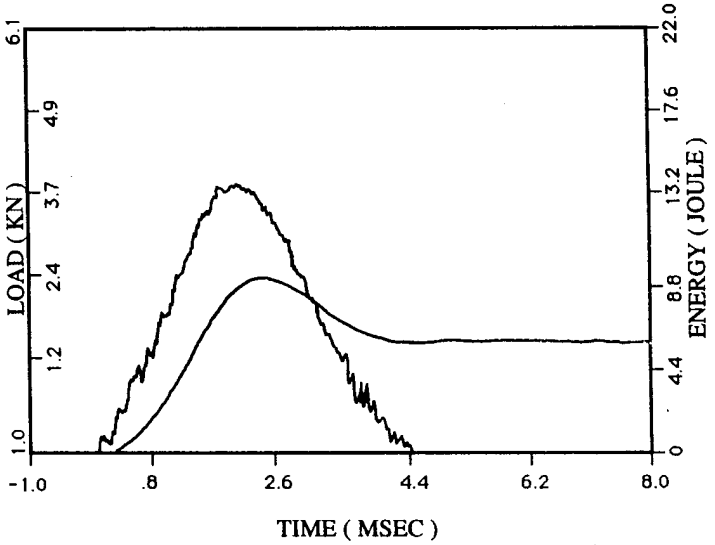


INSTRUMENTED OUTPUT

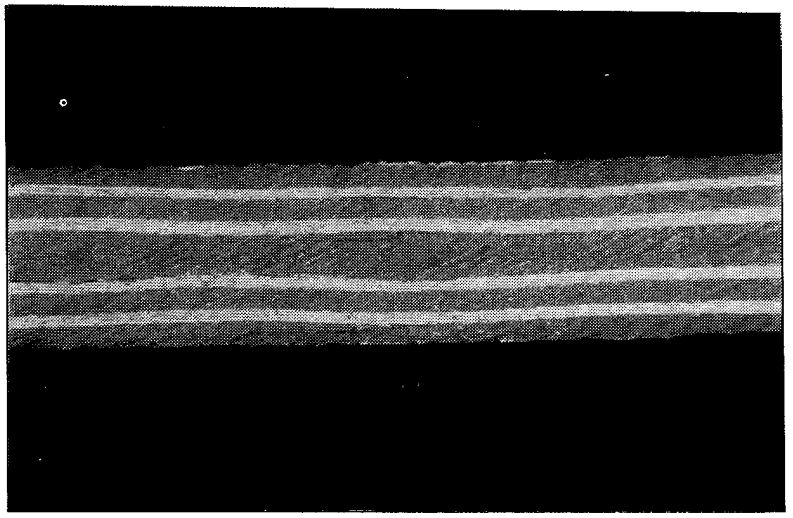

CROSS SECTION

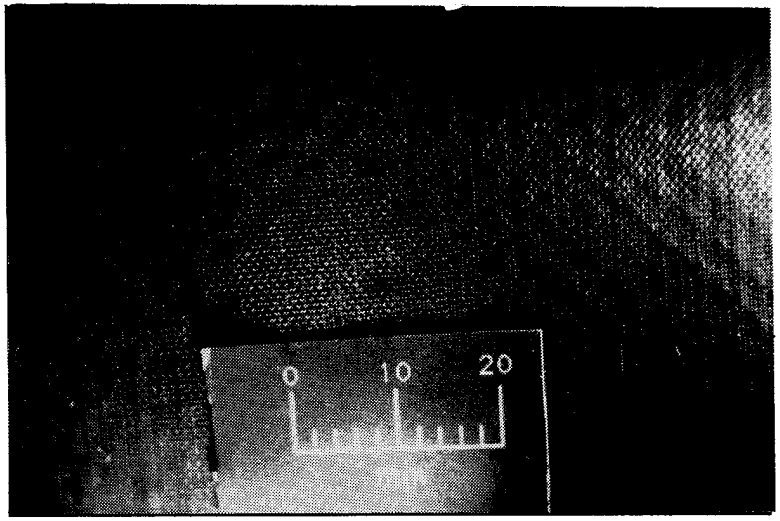


FRONT

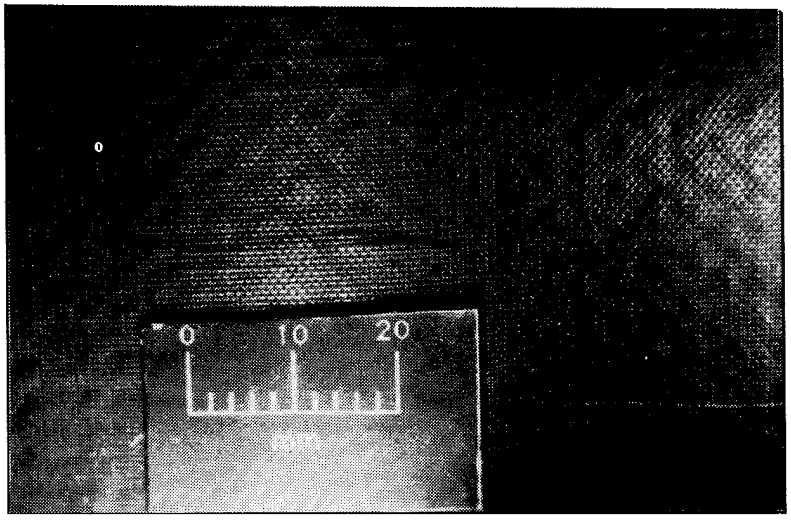


BACK

**IM7/1962 IMPACT ENERGY 9.2 J**

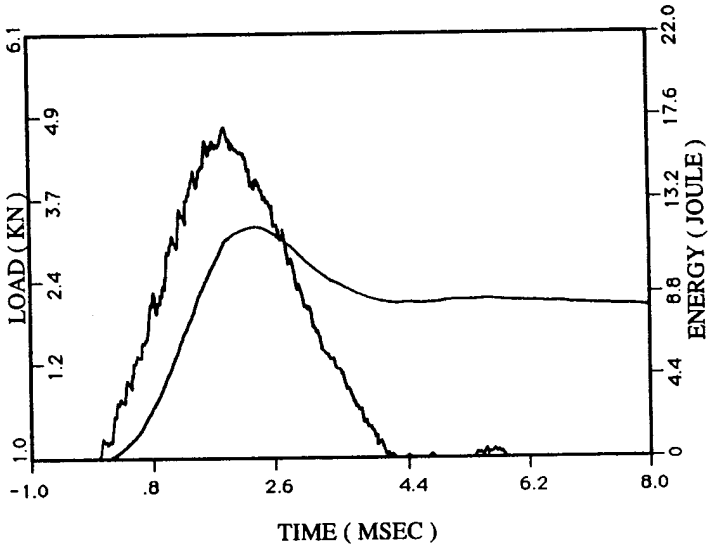


INSTRUMENTED OUTPUT

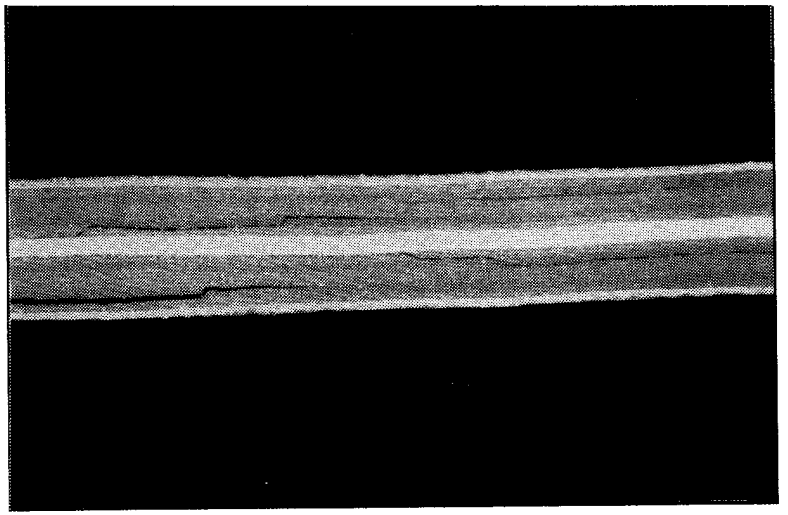

CROSS SECTION

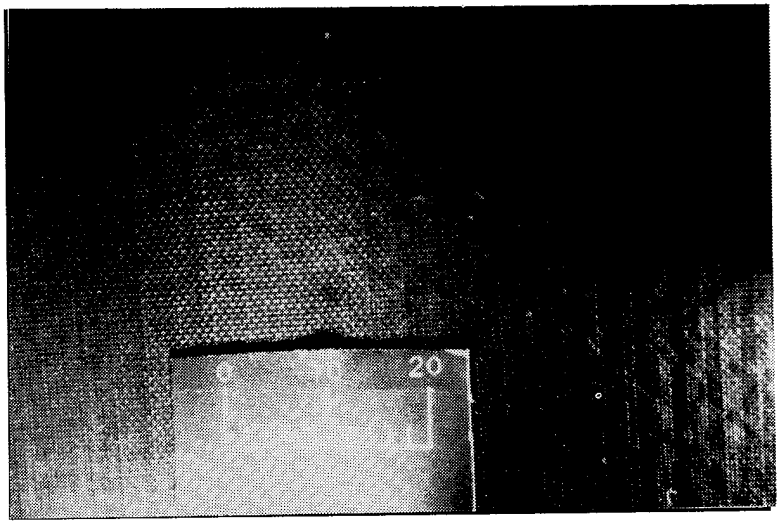

FRONT

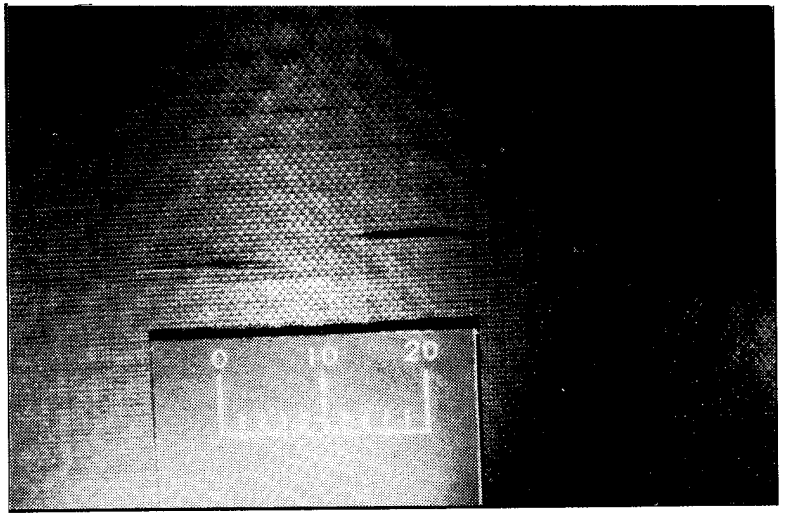

BACK

**IM7/1962 IMPACT ENERGY 12.2 J**

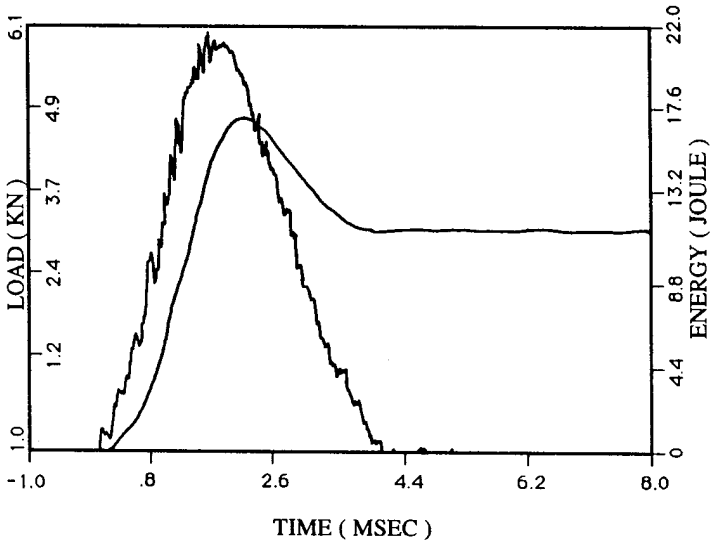


INSTRUMENTED OUTPUT

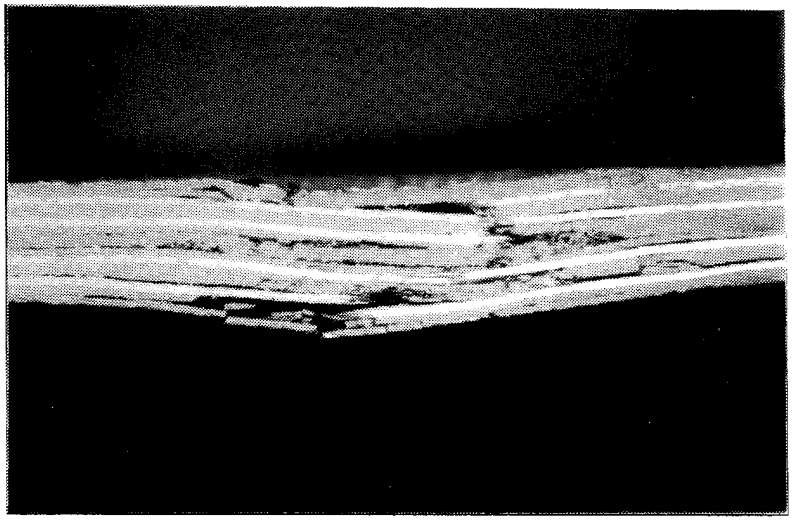

CROSS SECTION

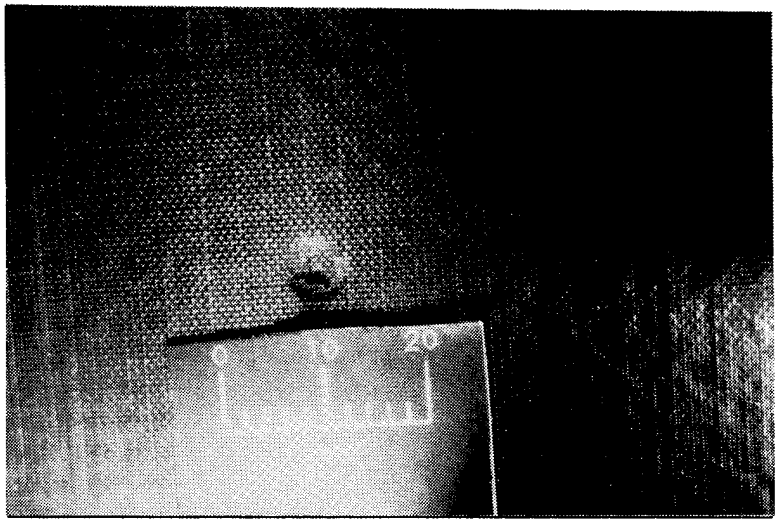


FRONT

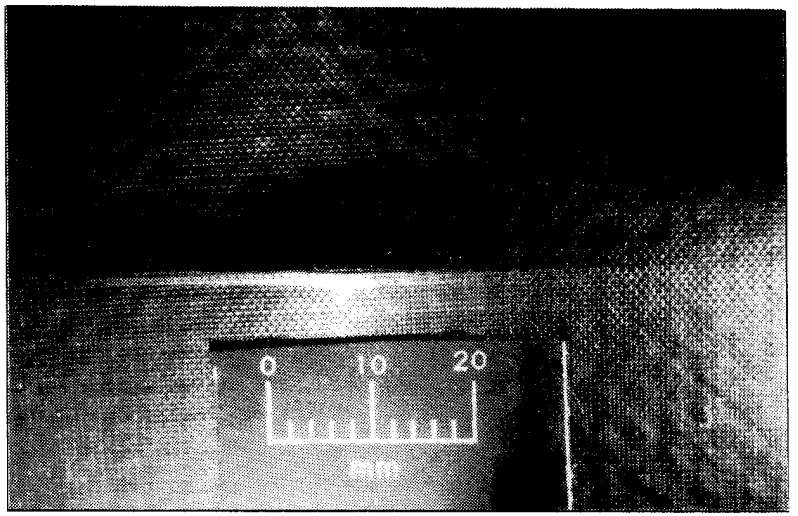


BACK

**IM7/1962 IMPACT ENERGY 17.2 J**

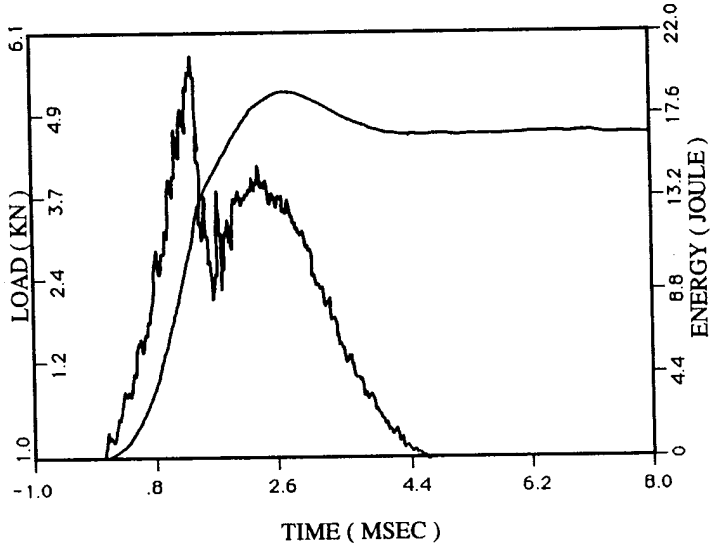


INSTRUMENTED OUTPUT

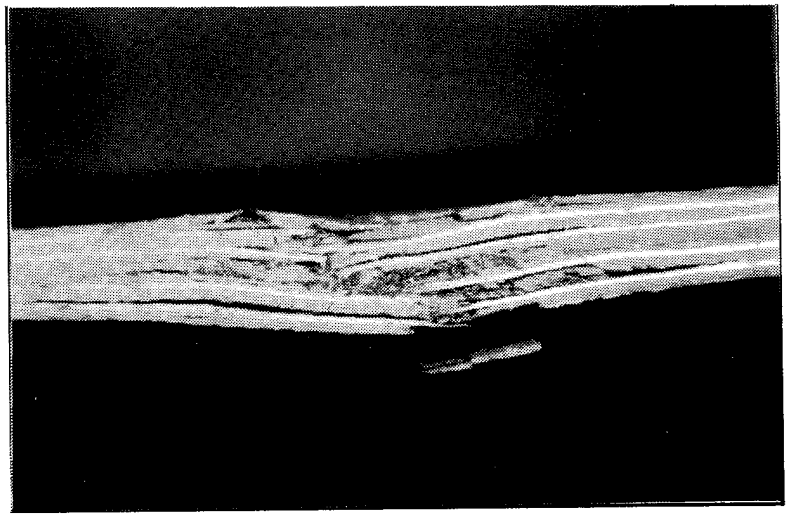

CROSS SECTION

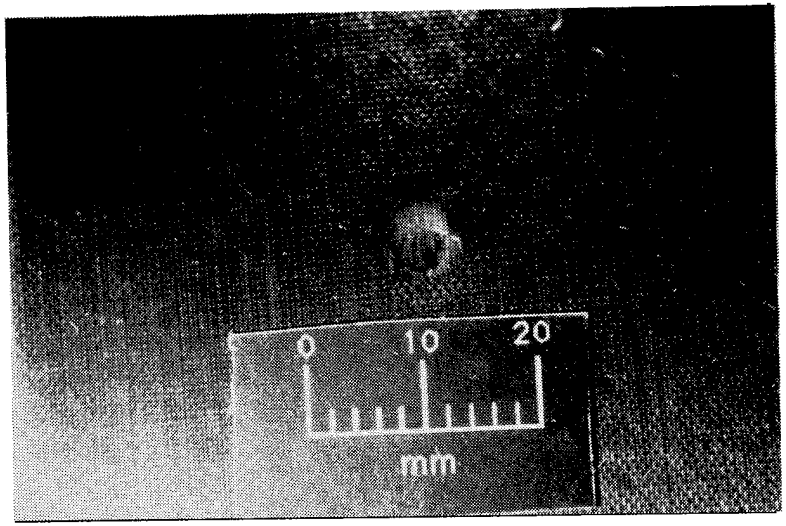


FRONT

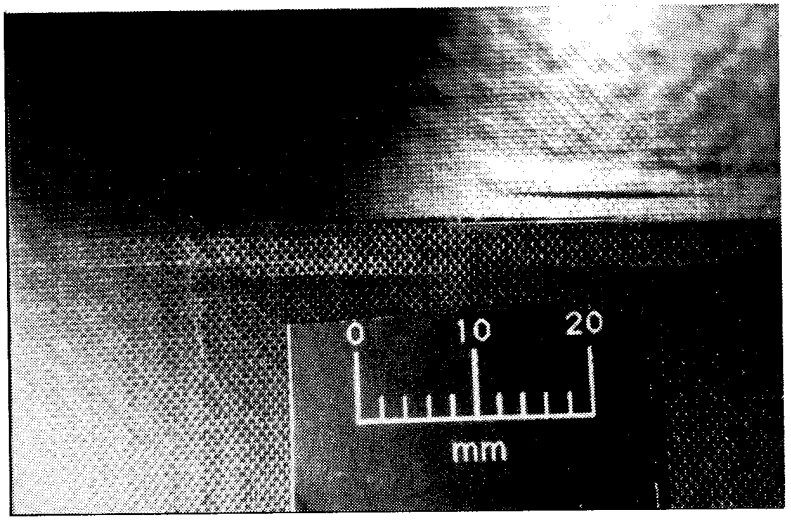


BACK

**IM7/1962 IMPACT ENERGY 19.1 J**

# APPENDIX B

## Cross-Sectional Photographs of the IM7/1939 Front Surface Cracks

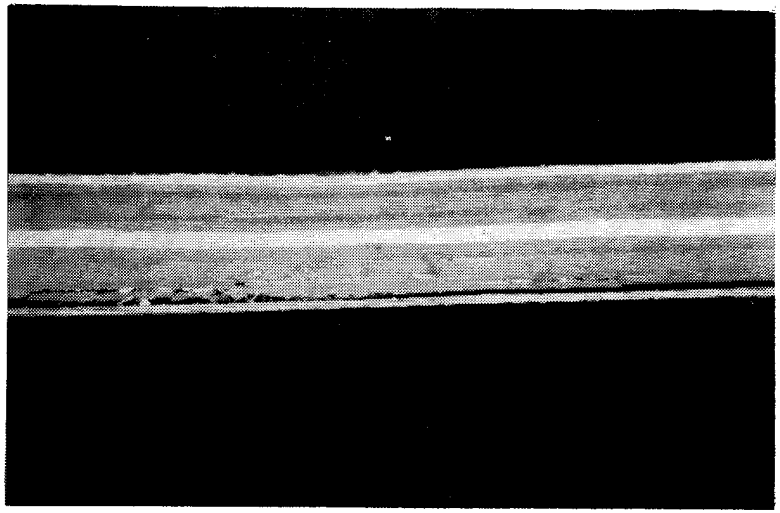

CROSS SECTION OF IMPACT SITE (10 x)

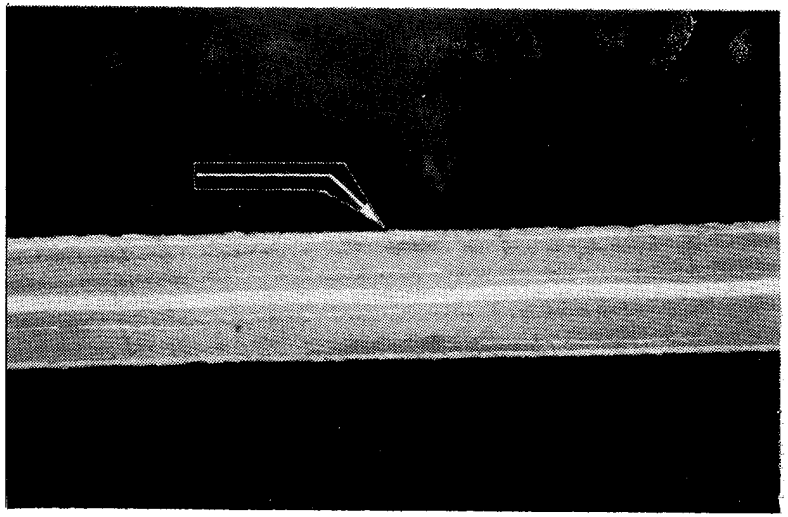

CROSS SECTION OF SURFACE CRACK (10 x)

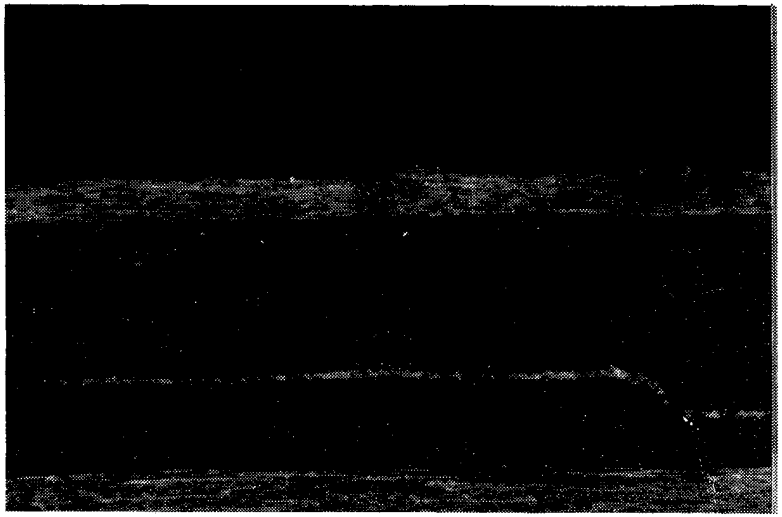

MAGNIFICATION OF SURFACE CRACK (50 x)

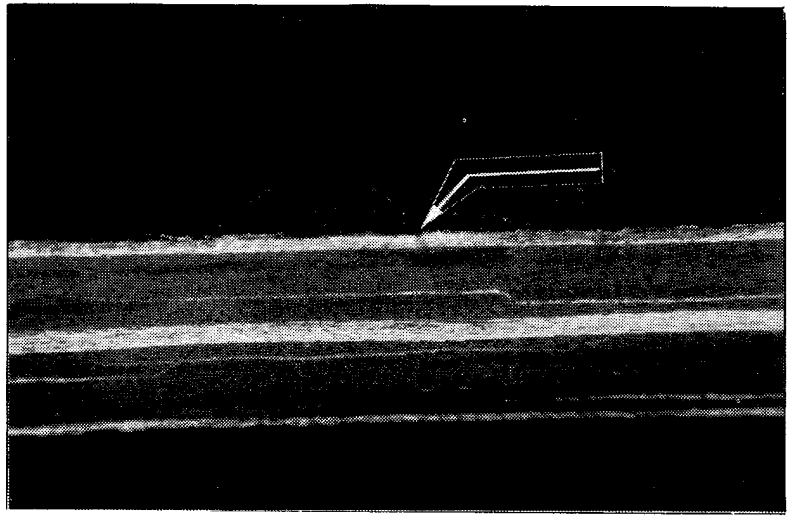

ANGLE VIEW OF SIDE AND TOP (16 x)

**IM7/1939 PERPENDICULAR CROSS-SECTIONAL CUT OF THE SURFACE CRACKS IMPACT ENERGY 9.1 J**

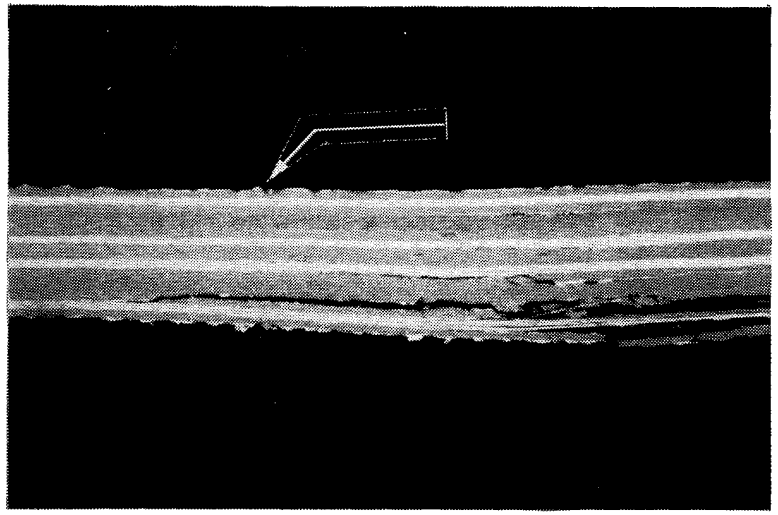

CROSS SECTION OF CRACK BESIDE IMPACT SITE (10 x)

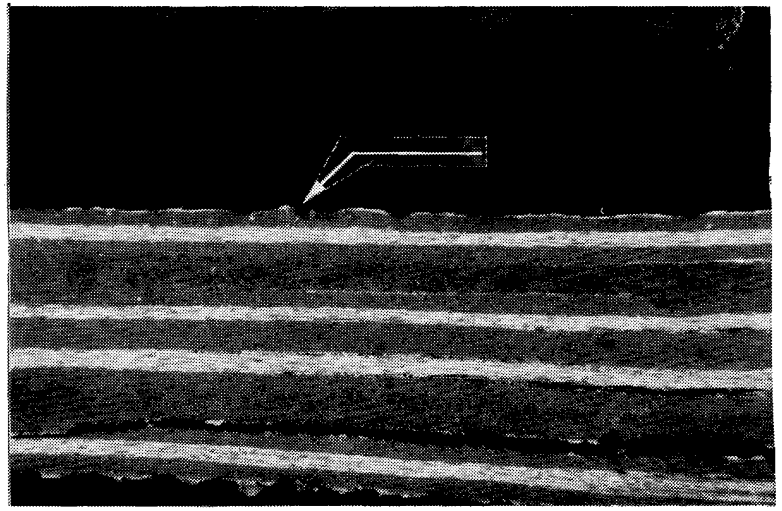

MAGNIFICATION OF CRACK (20 x)

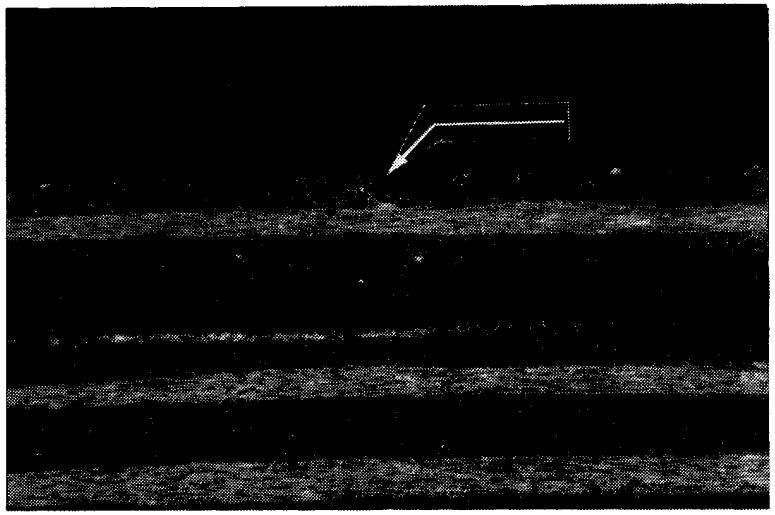

CROSS SECTION OF SURFACE CRACK (40 x)

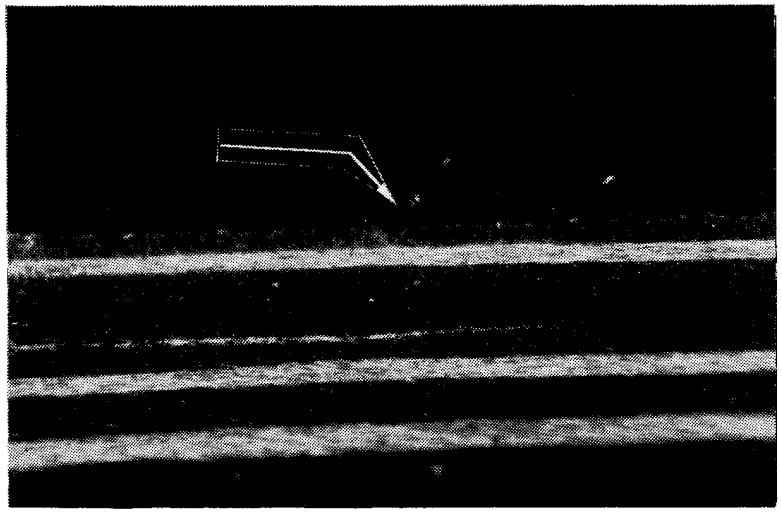

ANGLE VIEW OF SIDE AND TOP (32 x)

**IM7/1939 45° CROSS-SECTIONAL CUT OF THE SURFACE CRACKS**
**IMPACT ENERGY 12.2 J**

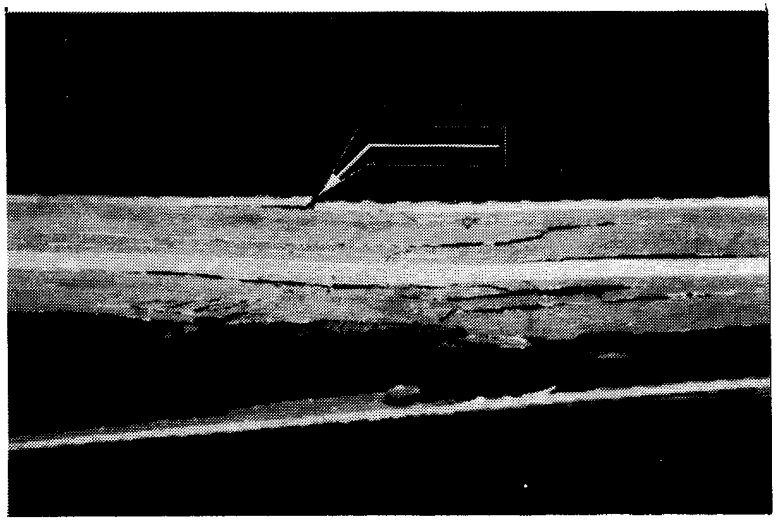

CROSS SECTION OF CRACK BESIDE IMPACT SITE (10 x)

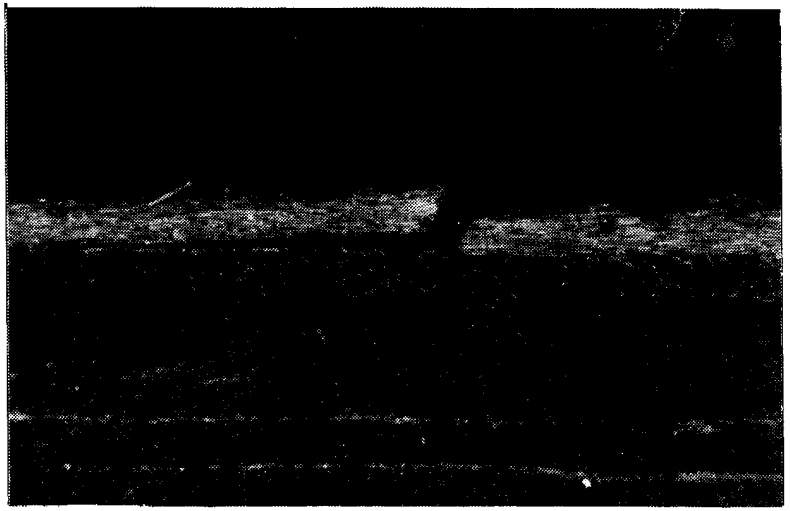

MAGNIFICATION OF CRACK (50 x)

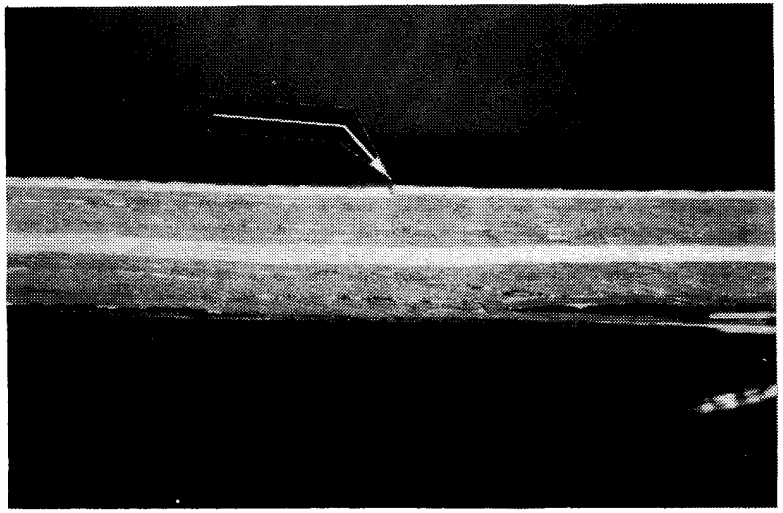

CROSS SECTION 2 mm FROM IMPACT (10 x)

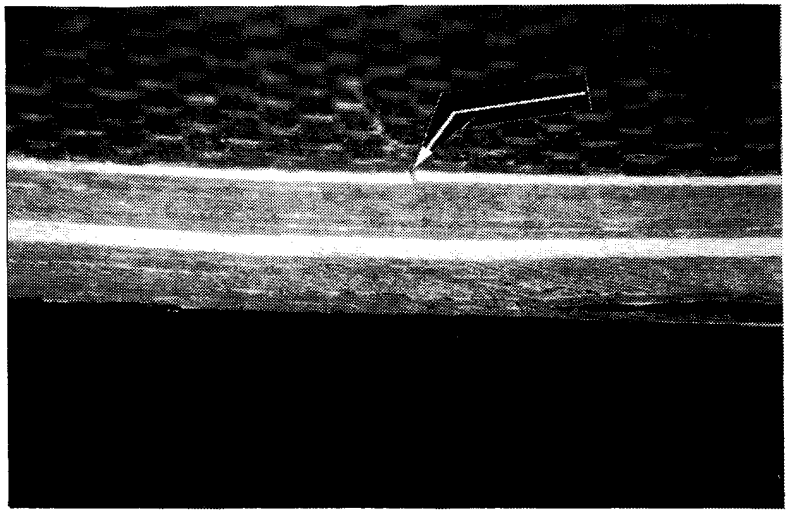

ANGLE VIEW OF SIDE AND TOP (12 x)

**IM7/1939 PERPENDICULAR CROSS-SECTIONAL CUT OF THE SURFACE CRACKS IMPACT ENERGY 17.2 J**

## REFERENCES


1. Winkel, J.D., and Adams, D.F.: "Instrumented Drop Weight Impact Testing of Cross-Ply and Fabric Composites." Composites Vol. 16, October 1985, pp. 268–278.

2. Aleska, J.C.: "Low Energy Impact Behavior of Composite Panels." Journal of Testing and Evaluation, Vol. 6, May 1978, pp. 202–210.

3. Sjoblom, P.O., Harntess, J.T., and Cordell, T.M.: "On Low-Velocity Impact Testing of Composite Materials." Journal of Composite Materials, Vol. 22, January 1988, pp. 30–52.

4. Nettles, A.T.: "Instrumented Impact and Residual Tensile Strength Testing of Eight-Ply Carbon/Epoxy Specimens." NASA TP 2981, January 1990.

5. Chang, F.K., Choi, H.Y., and Jeng, S.T.: "Characterization of Impact Damage in Laminated Composites." SAMPE Journal Vol. 26, No. 1, January/February 1990.

6. Stellbrink, K.: "Examination of Impact Resistance of FRP-Suggestion for a Standard Test Method." Mechanical Characterization of Load Bearing Fiber Composites and Laminates. Elsevir Applied Science Publishers, A.H. Cardon and C. Verchery eds., London and New York.

7. Cantwell, W.J., and Morton, J.: "Detection of Impact Damage in CFR Laminates." Composite Structures, Vol. 3, 1985, pp. 241–257.

8. Cantwell, W.J., Curtis, P.T., and Morton, J.: "An Assessment of the Impact Performance of DFRP Reinforced With High-Strain Carbon Fibers." Composite Science and Technology, Vol. 25, No. 2, 1986, pp. 133–148.

9. Wyrick, D.A., and Adams, D.F.: "Damage Sustained by a Carbon/Epoxy Composite Material Subjected to Repeated Impact." Composites, Vol. 19, No. 1, January 1988.

NASA
National Aeronautics and Space Administration

# Report Documentation Page

| 1. Report No. | 2. Government Accession No. | 3. Recipient's Catalog No. |
|---|---|---|
| NASA TP-3029 | | |

| 4. Title and Subtitle | 5. Report Date |
|---|---|
| Low Velocity Instrumented Impact Testing of Four New Damage Tolerant Carbon/Epoxy Composite Systems | July 1990 |
| | 6. Performing Organization Code |

| 7. Author(s) | 8. Performing Organization Report No. |
|---|---|
| D.G. Lance and A.T. Nettles | |
| | 10. Work Unit No. M-636 |

| 9. Performing Organization Name and Address | 11. Contract or Grant No. |
|---|---|
| George C. Marshall Space Flight Center<br>Marshall Space Flight Center, Alabama 35812 | |
| | 13. Type of Report and Period Covered |
| 12. Sponsoring Agency Name and Address | Technical Paper |
| National Aeronautics and Space Administration<br>Washington, D.C. 20546 | 14. Sponsoring Agency Code |

15. Supplementary Notes

Prepared by Materials and Processes Laboratory, Science and Engineering Directorate.

16. Abstract

Low velocity drop weight instrumented impact testing was utilized to examine the damage resistance of four recently developed carbon fiber/epoxy resin systems. A fifth material, T300/934, for which a large data base exists, was also tested for comparison purposes. A 16-ply quasi-isotropic lay-up configuration was used for all the specimens. Force/absorbed energy-time plots were generated for each impact test. The specimens were cross-sectionally analyzed to record the damage corresponding to each impact energy level. Maximum force of impact versus impact energy plots were constructed to compare the various systems for impact damage resistance. Results show that the four new damage tolerant fiber/resin systems far outclassed the T300/934 material. The most damage tolerant material tested was the IM7/1962 fiber/resin system.

| 17. Key Words (Suggested by Author(s)) | 18. Distribution Statement |
|---|---|
| Composite Materials<br>Epoxy Resins<br>Damage Tolerance<br>Instrumented Impact Testing | Unclassified–Unlimited<br>Subject Category: 24 |

| 19. Security Classif. (of this report) | 20. Security Classif. (of this page) | 21. No. of pages | 22. Price |
|---|---|---|---|
| Unclassified | Unclassified | 40 | A03 |

**NASA FORM 1626** OCT 86

For sale by the National Technical Information Service, Springfield, VA 22161-2171

NASA-Langley, 1990